Scale Resolving Simulations of Corner-Flow Separation in a Wing-Fuselage Juncture

Aditya Ghate, Jeffrey Housman

Gerrit-Daniel Stich, Gaetan Kenway & Cetin Kiris

Computational Aerosciences Branch,

NASA Ames Research Center

Advanced Modeling & Simulation (AMS) Seminar Series

NASA Ames Research Center, September 10, 2020

Part of this material was presented before at AIAA Aviation, 2020

AIAA-2020-2375

Scale-resolving simulations – Background

- Limited success of steady state RANS (including SMCs) for problems where mean-flows are strongly influenced by dynamics of large scales of turbulence (Chaouat, 2017)
  - Struggle with predictive RANS of juncture flows was acknowledged in past AIAA workshops (DPW, HLPW, etc.)
- LES captures geometry/boundary influenced large scales but has a prohibitive cost scaling for TBLs (Spalart, 1997; Choi & Moin, 2012)
- Methods that combine advantages of RANS and LES are naturally suited to handle high Reynolds number non-equilibrium wall turbulence (Cabot & Moin, 1999; Spalart, 2000)
- Rapid growth of interest in hybrid approaches

Change in annual papers published on "hybrid-RANS/LES"

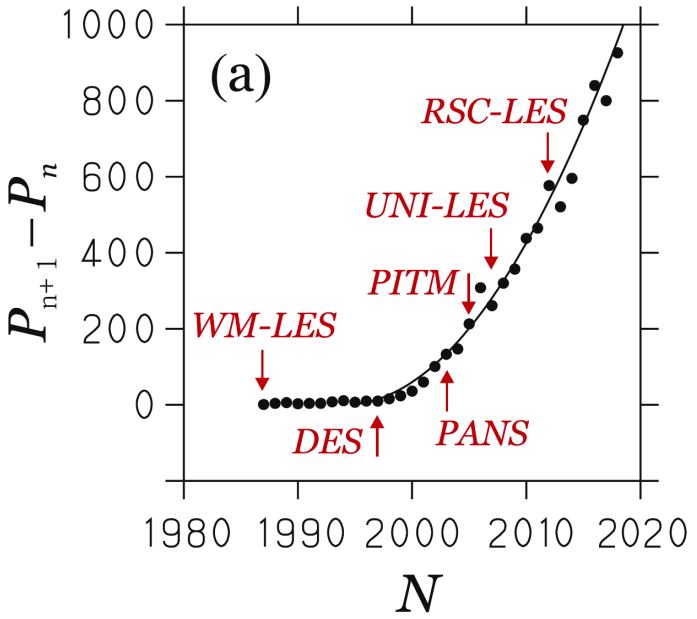
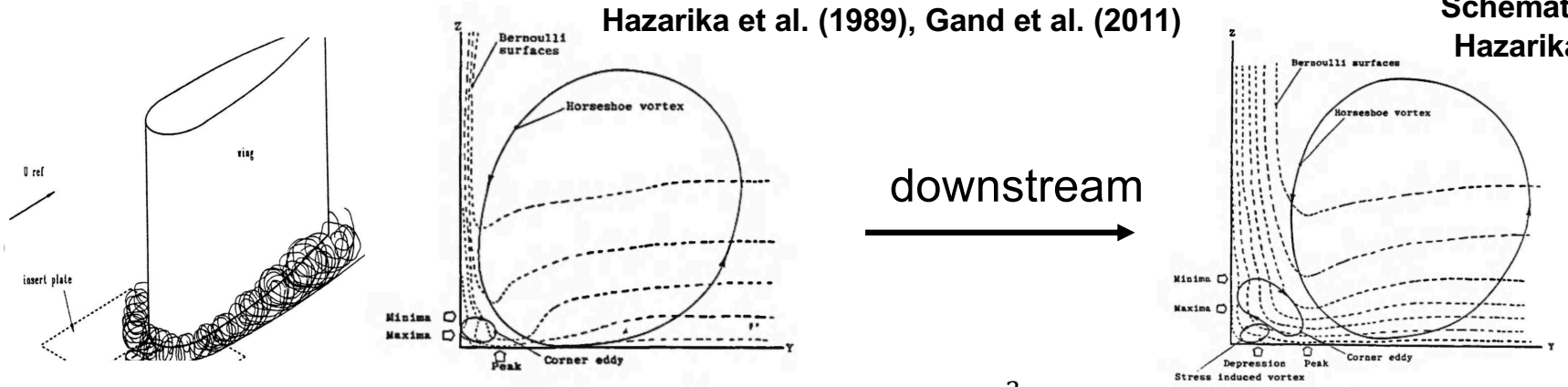


Figure taken from Heinz (2020), *Progress in Aerospace Sciences*

Corner/junction flows – Background

Phenomenology by Perkins (1970), Hazarika et al. (1989), Gand et al. (2011)

Schematics taken from Hazarika, et al. (1989)

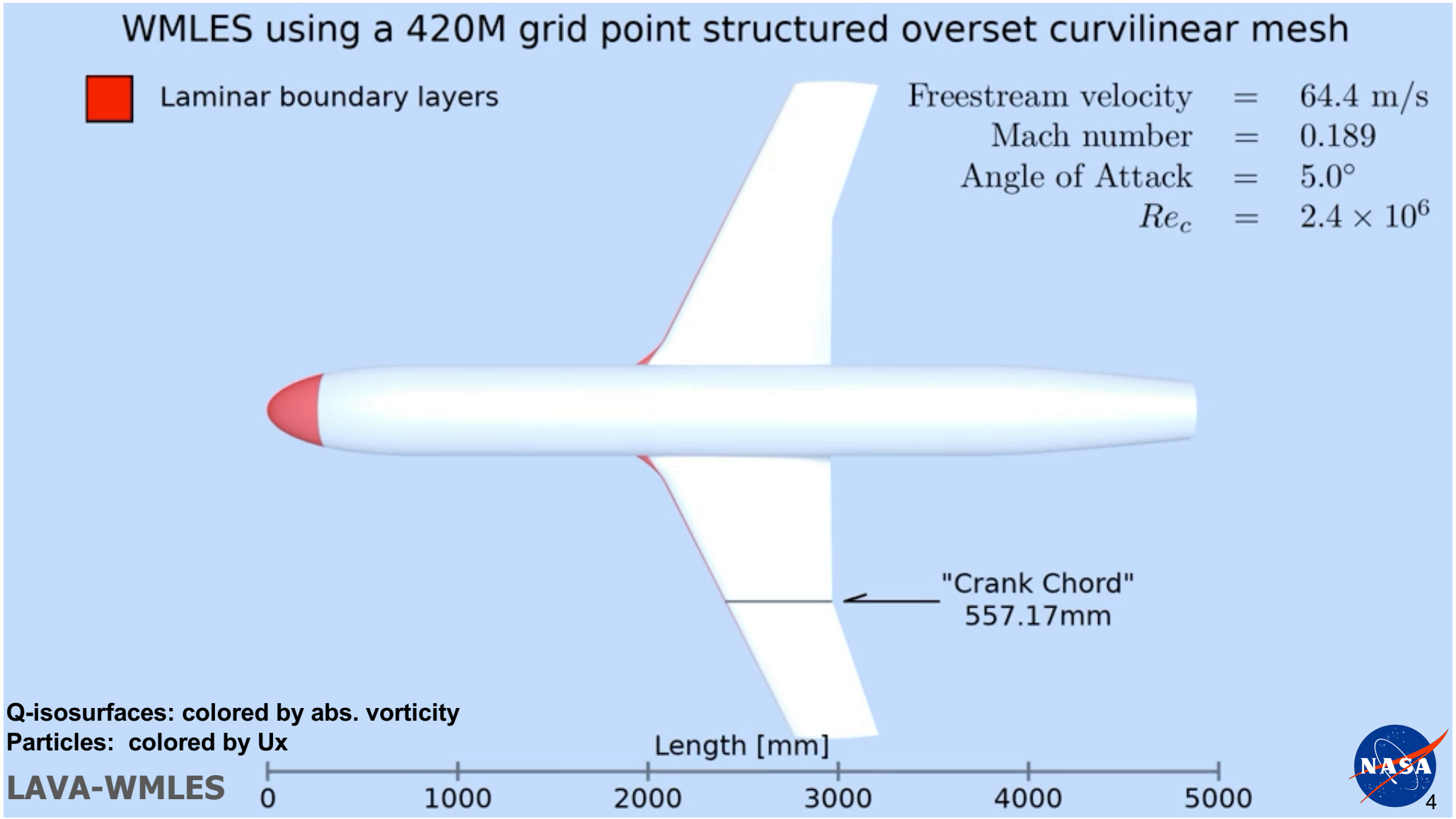


- Problem with linear eddy viscosity closures ($\tau_{ij} = -2\nu_t S_{ij} + \frac{2}{3}k\delta_{ij}$) – no secondary flow permitted

$$u\partial_x\omega_x + v\partial_y\omega_x + w\partial_z\omega_x = \left(\partial_y\partial_y - \partial_z\partial_z\right)\tau_{23} + \partial_y\partial_z\left(\tau_{22} - \tau_{33}\right)$$
$$+\partial_x\left(\partial_z\tau_{12} - \partial_y\tau_{13}\right) + \text{viscous diffusion} + \text{vortex stretching}$$

  - Non-linear corrections (such as Spalart's QCR) are needed
  - Rumsey et al. (2017-2020) have reported some success with QCR for juncture flow
  - Recent work by Modesti (2020) did a-priori analysis for duct flow in terms of Pope's (1975) general tensor expansion; showed **promising agreement for QCR-2000**

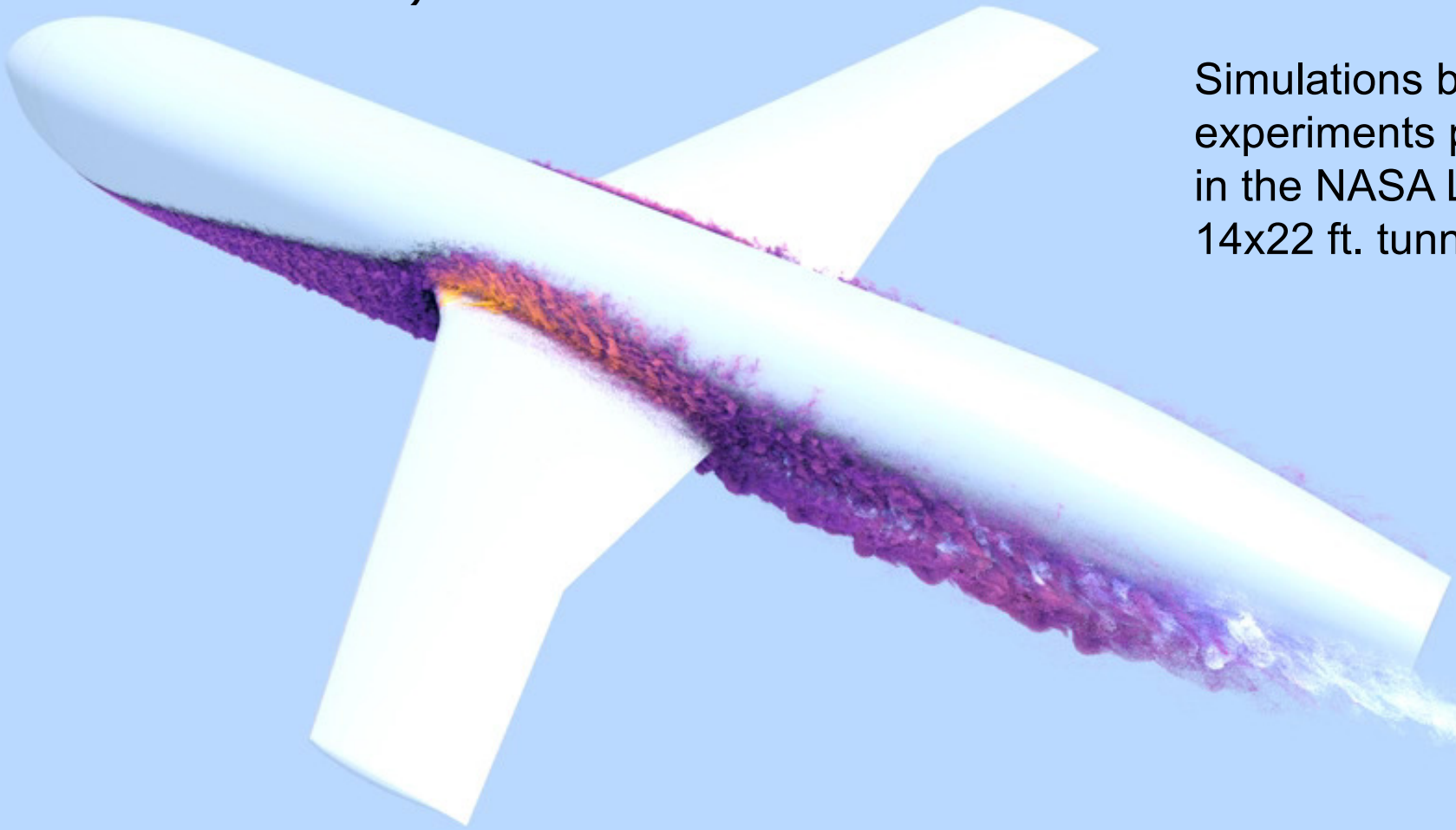
WMLES using a 420M grid point structured overset curvilinear mesh



Q-isosurfaces: colored by abs. vorticity
Particles: colored by Ux

LAVA-WMLES

Visualization generated by: Timothy Sandstrom
(NASA Ames Research Center)



Simulations based on experiments performed in the NASA Langley 14x22 ft. tunnel

LAVA-WMLES

Outline

- DDES and known deficiencies
- WMLES and known deficiencies
- Structured curvilinear overset grid systems
- Numerical scheme
- Results – comparisons with experiment*
- Computational Cost
- Summary

*Comparisons made with experimental measurements (LDV) by **Kegerise & Neuhart (2019)**

DDES

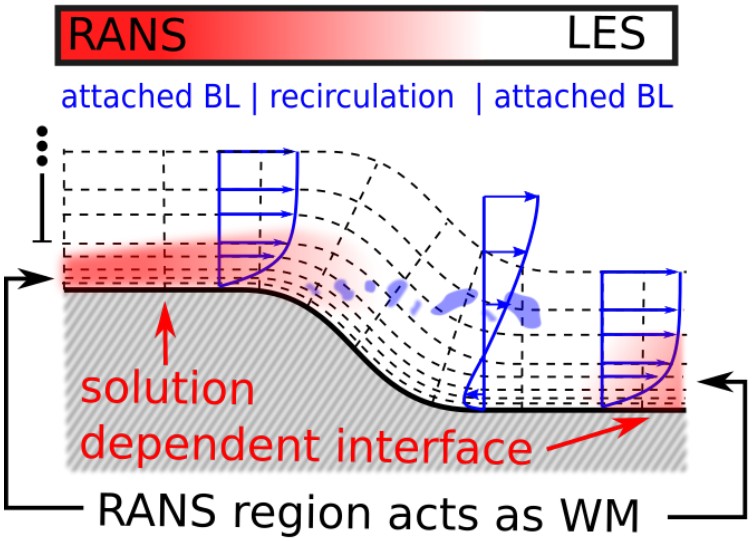
- **Basic philosophy:**

  Would like to use RANS everywhere, but no robust model for separated flows; so switch to LES in free-shear layers and separated flows (detached boundary layers)

- Success of the method relies on a robust "indicator function" which informs the switch to LES
- Present work uses Deck's (2012) Mode-II definition

$$f_d = 1 - tanh\left(\left[8\frac{\nu + \nu_t}{\sqrt{U_{i,j}U_{i,j}\kappa^2 d_w^2}}\right]^3\right)$$

$$d_{ddes} = d_w - f_d \max\left(0, d_w - C_{DES}\Delta_{\text{vol}}\right)$$

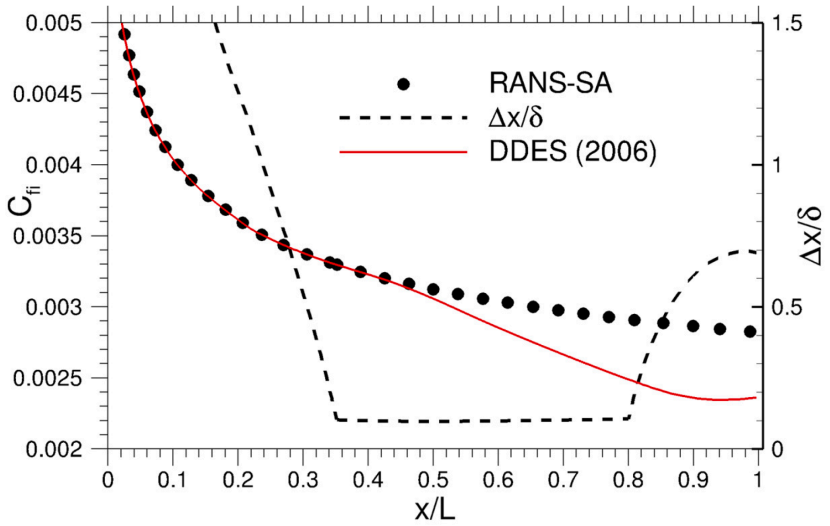


- Present work uses cube-root-volume for LES length scale, although alternate vorticity-based form available

DDES

- **Known failure mechanism:** Modelled Stress Depletion (MSD)
  - Indicator function detects a switch to LES for attached boundary layers if $\delta_{BL} > C_{\mathrm{DES}}\Delta_x$
  - Lack of any resolved turbulence results in sudden drop in total stress
  - Unphysical TBL profiles result and cause a drop seen in skin friction for flat plate BLs

Figure taken from Deck et al., 2020



- Recent solution by Deck et al. (2020) appears to be a promising
- Other Hybrid-RANS/LES techniques such as ZDES were tested initially; adequate resolution requirements were cost-prohibitive

WMLES

- **Basic philosophy:**

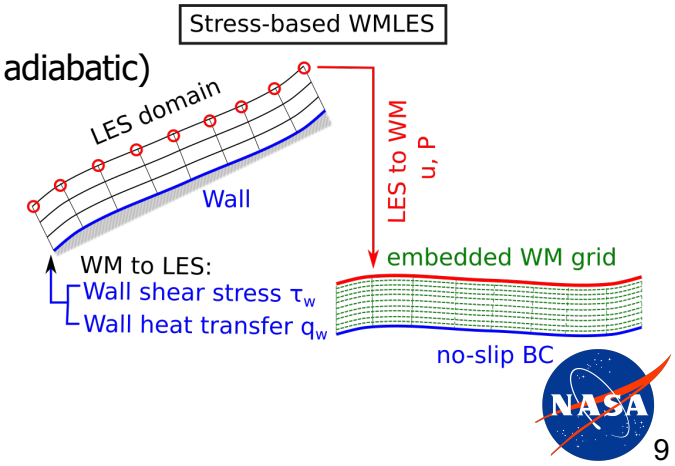
  Would like to use LES everywhere but cannot resolve integral length scales for the inner-layer of a TBL at high Reynolds numbers; so use replace stiff-Dirichlet BCs with a wall-stress BC instead and compute the wall-stress using a RANS model.

- Basic principle first introduced in 70s and 80s (Deardorff, Schumann, Moeng, etc.) for atmospheric boundary layers; stress computed using wall-functions for rough-walls
- Idea generalized for engineering flows by solving TBLE to predict wall-stress (Balaras & Benocci, 1994; Cabot & Moin, 2000; Kawai & Larsson, 2013; Park & Moin, 2014)
- Recent reviews by Larsson et al. (2016) and Bose & Park (2018) cover other alternate formulations
- Success of the method relies **on numerical discretization and SGS closure beyond just the wall-model**
- **Equilibrium assumption** simplifies the TBLE to a system to an ODE (low-Mach, adiabatic)

$$\frac{d}{dy}\left[\left(\nu + \nu_t(y)\right)\frac{du}{dy}\right] = 0$$

- Instead of assuming a damping law (van-Driest for example) for $\nu_t(y)$, one can directly assume an **algebraic solution** (wall-function) to the ODE

$$u^+ = f(y^+)$$



WMLES

- **Challenges related to corner flows:**
  - Exchange location typically 2nd off-wall compute point or higher; issue at corners
  - Is the non-equilibrium physics in the corner sufficiently resolved for equilibrium WM?
  - Vane & Lele (2015) proposed modifications to matching location (Buleev); however showed sensitivity to eddy viscosity model
  - Recent work (Wu et al., 2018) suggests damping SGS constant near corners alleviates the issue
  - Ongoing work on development of RANS-informed SGS closure near-corner (inspired by Shiyi Chen's CLES)
- **Present formulation:**
  - Algebraic WM based on Musker's wall-function; heat transfer using Kader-law (inapplicable if adiabatic)
  - Exchange location at second off-wall compute node
  - Additional considerations needed for node-based discretizations

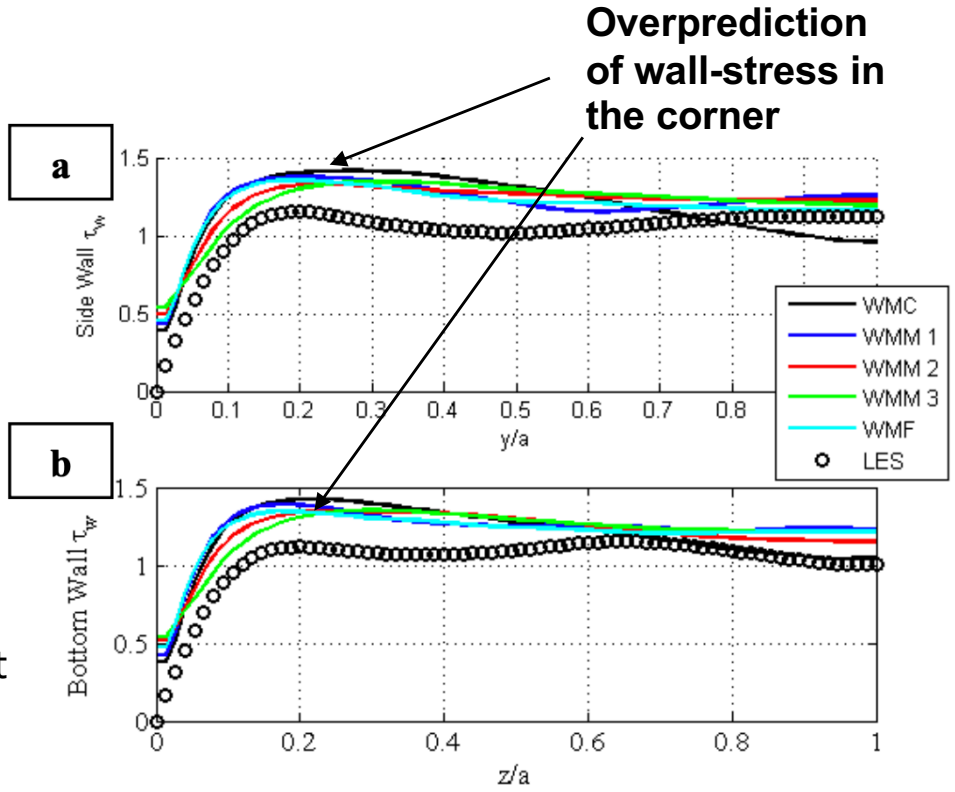


Figure taken from Vane & Lele, AIAA, 2015

Overset Grid System

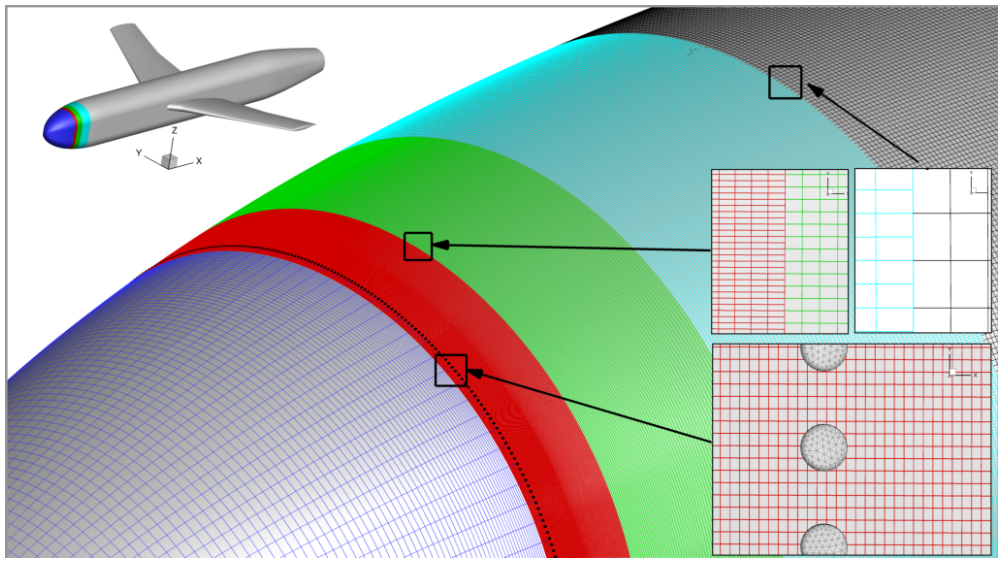
- Grid system used for RANS is re-used for DDES*
  - Medium and Fine RANS meshes satisfy the DDES grid quality criteria (Spalart et al., 2006)
  - Preliminary studies with physics-informed DDES meshes did not produce qualitative differences
  - Industry usage of DDES typically relies on RANS-type meshing with no attention to LES requirements

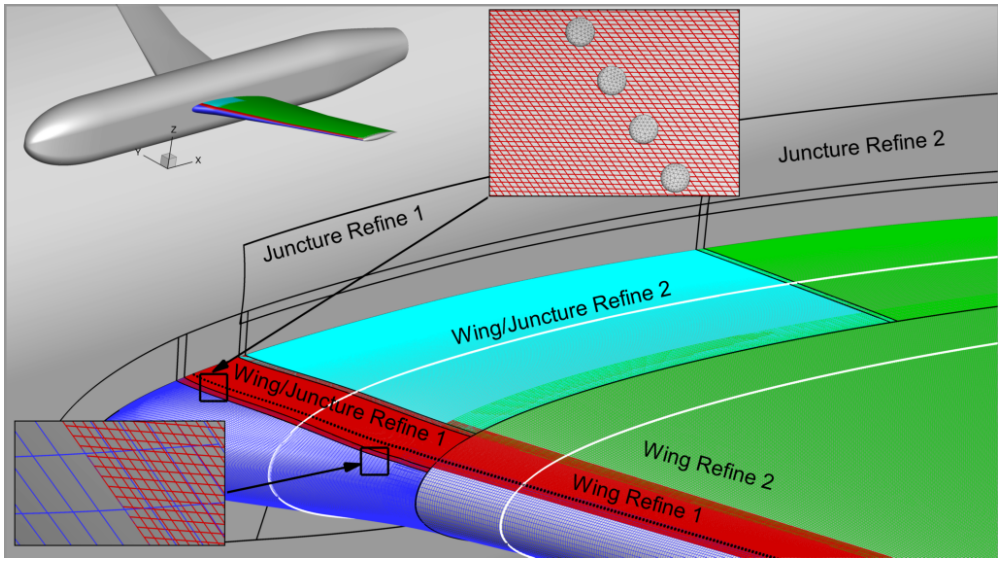
- Early attempts at ZDES (Mode III) were projected to use > 1E9 grid points due to both y+ and span & stream spacing restrictions (similar grid requirements expected for IDDES)

*** RANS meshes generated by Henry Lee (ARC); Lee & Pulliam (AIAA-2019-0080)**

Overset Grid System for WMLES

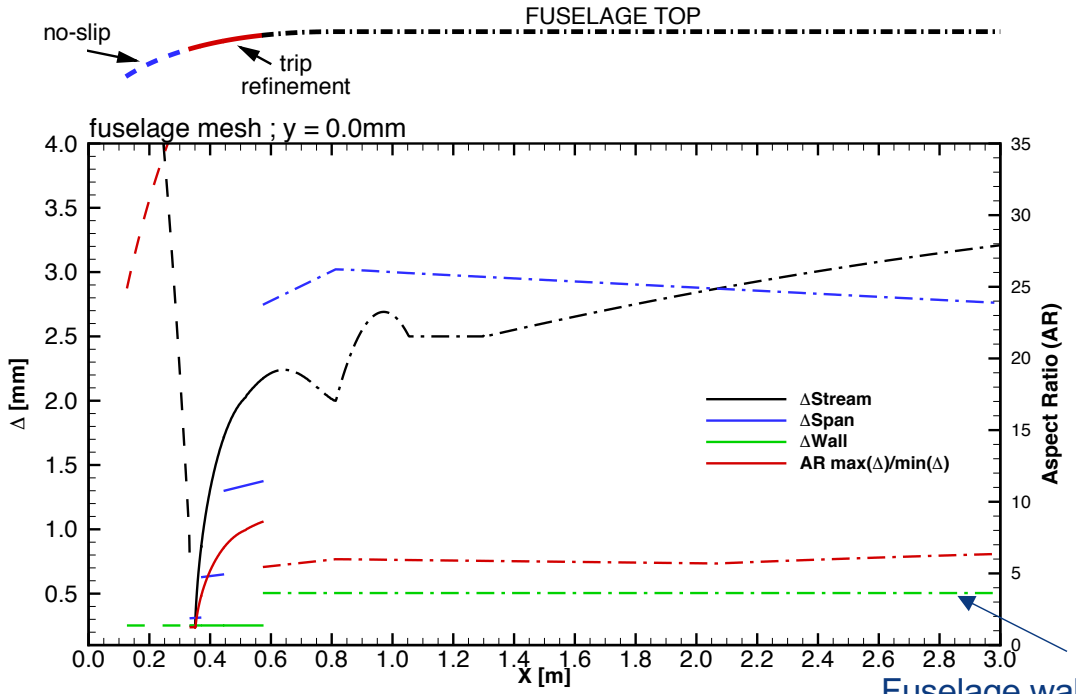
- Both fuselage and wing tripping represented; early boundary layer growth resolved according to "points-per-delta" based metrics (Larsson et al., 2016)
- Tripping dots represented using a penalty (immersed boundary) method

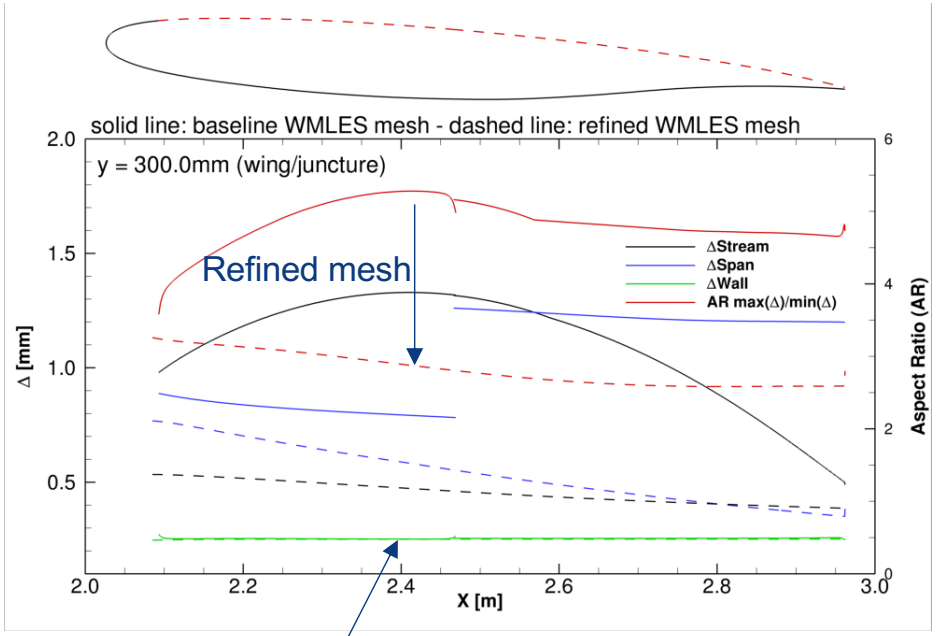




Overset Grid System for WMLES

- Aspect ratios constrained to stay under 7 across the fuselage
- Refined mesh to reduce the streamwise spacing and decrease aspect ratio to <3



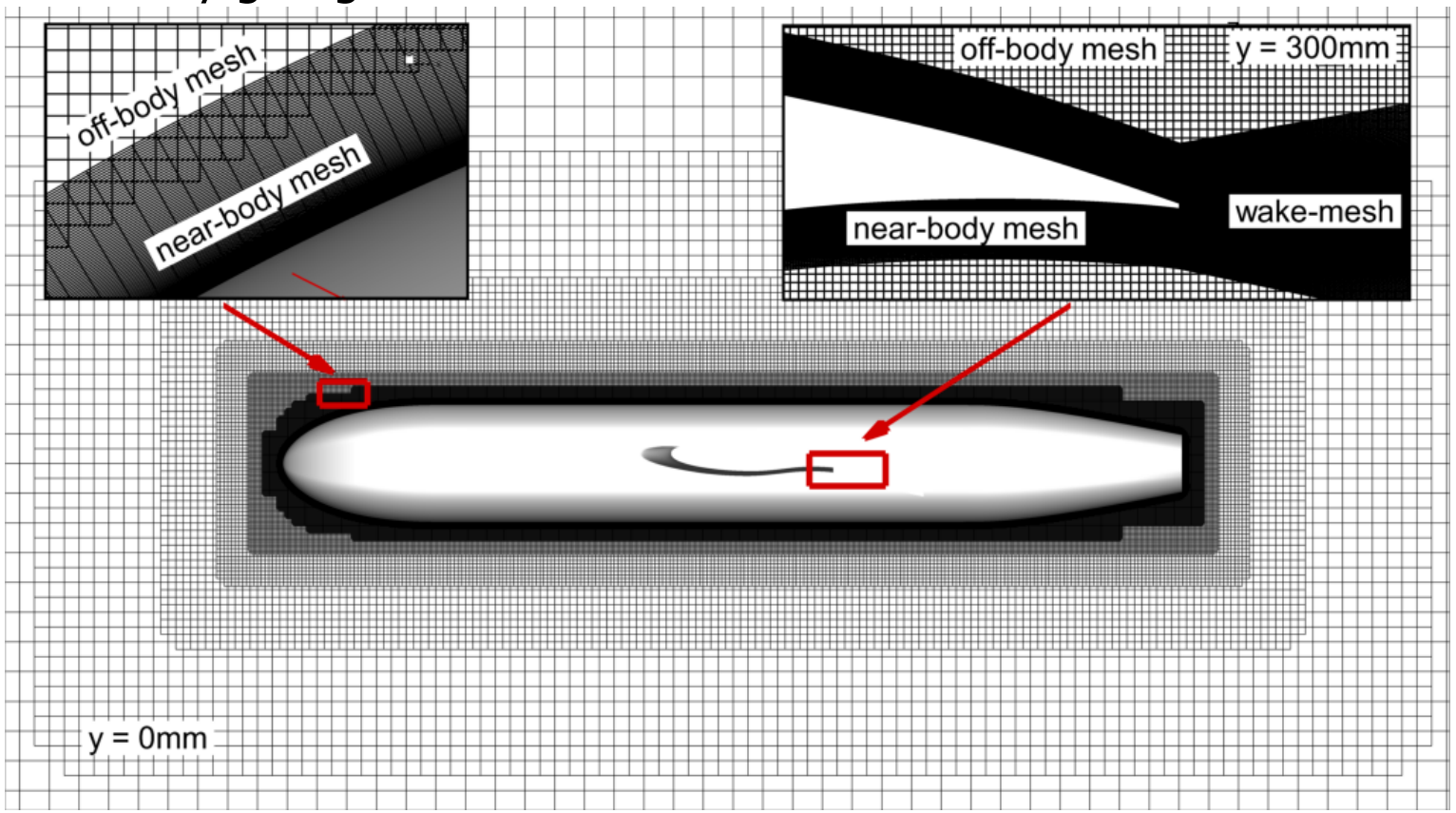


Fuselage wall spacing: 0.50mm

Juncture region wall spacing: 0.25mm

Overset Grid System for WMLES

- Off-body grid generated as a Cartesian overset mesh



Overset Grid System

- Summary of overset grid systems simulated (full-span)

Mesh Type	Fuselage	Wing	Near-body	Off-body	Total Points
RANS/DDES coarse mesh	2.7	16.2	19.3	5.0	23.9
RANS/DDES medium mesh	10.3	37.6	47.9	8.9	56.8
RANS/DDES fine mesh	48.5	119.8	168.3	28.6	196.9
Baseline WM-RANS mesh	129.0	86.8	215.8	82.0	297.8
Baseline WM-LES mesh	129.0	228.5	357.5	82.5	440.0
Refined WM-LES mesh	129.0	297.4	462.4	82.5	509.4

***Numbers reported are in million grid points**

WM-RANS results reported in AIAA-2020-2735

Numerical discretization

- Convective flux discretization uses
  - Primitive variable interpolation to the half-points
    - Blending between 2nd order centered and 1st order upwind
    - Blending between 4th order centered and 3rd order upwind
  - Modified version of Roe numerical flux (Housman et al., 2009)
- Nodal flux derivative uses 2nd order central (staggered) or 4th order combined nodal/staggered differentiation
- Time discretization using BDF2 for DDES
  - Uses a dual-time stepping scheme
  - Linearized system solved with ILU(0)-GMRES
- Time discretization using TVD-RK3 for WMLES
- More details provided in AIAA-2020-2735

Comparisons with experiment

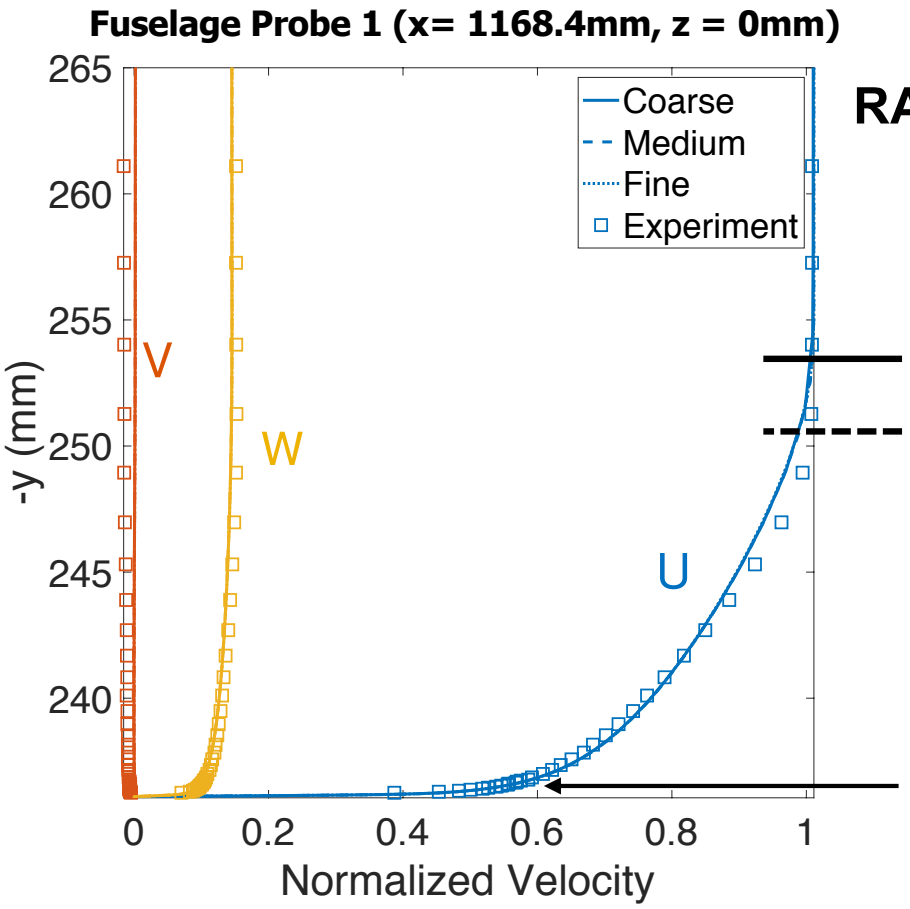
- Comparisons with LDV probes
  - Velocity profiles
  - Cross-correlations (cross-stresses, single-point) – Resolved+Modeled components
  - Variances (normal stresses, single-point) – Resolved components
- Sectional pressure coefficient (c_p)
  - Only the most inboard section considered
  - All simulations are accurate for all outboard stations, except near wing tips
- Steady state RANS simulations using **SA-RC-QCR2020** (Rumsey et al., AIAA J., 2020) used as reference to assess improvements over RANS

Probes considered for analysis:

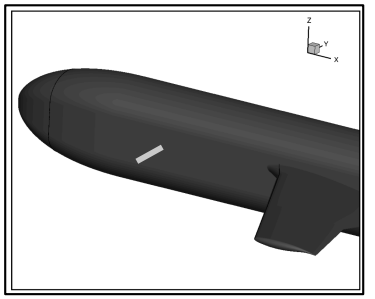
- 1 probe on the fuselage
- 2 probes in the horn region
- 15 probes in the juncture region

Only a **subset** discussed in subsequent slides

Fuselage probe



RANS (SA-RC-QCR2020)

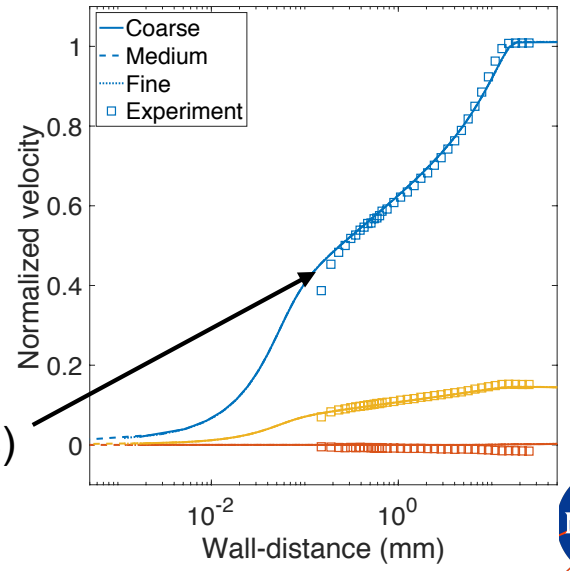


- No-grid sensitivity seen in the fuselage boundary layer
- RANS simulations **are not tripping-aware**

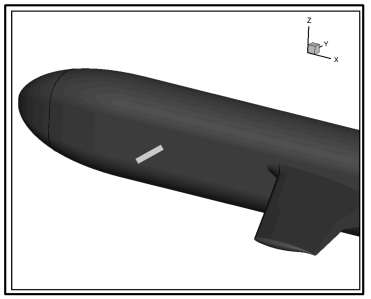
RANS BL thickness: 24 mm

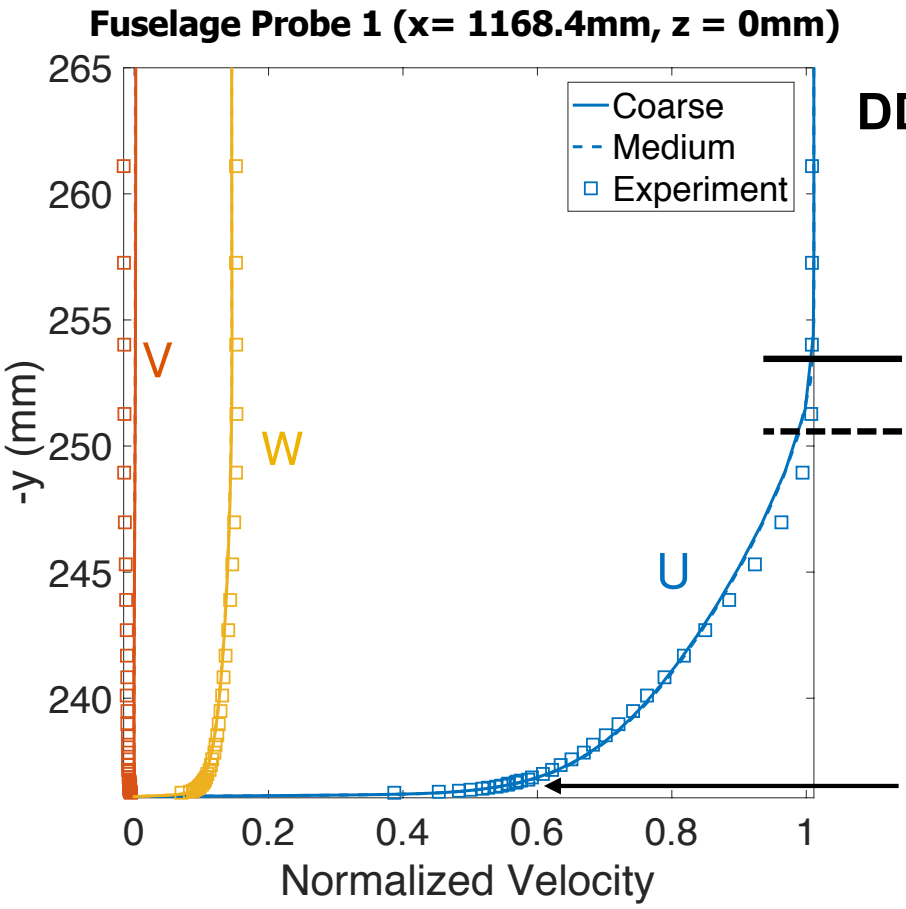
Experiment BL thickness: 20 mm

Accurate inner-layer (correct c_f predictions)



Fuselage probe





DDES (SA-RC-QCR2000)

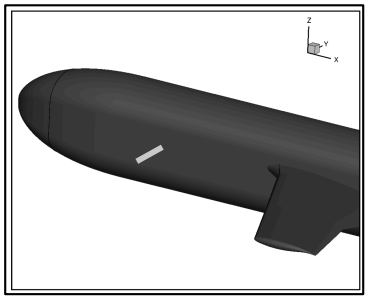
DDES BL thickness: 24 mm

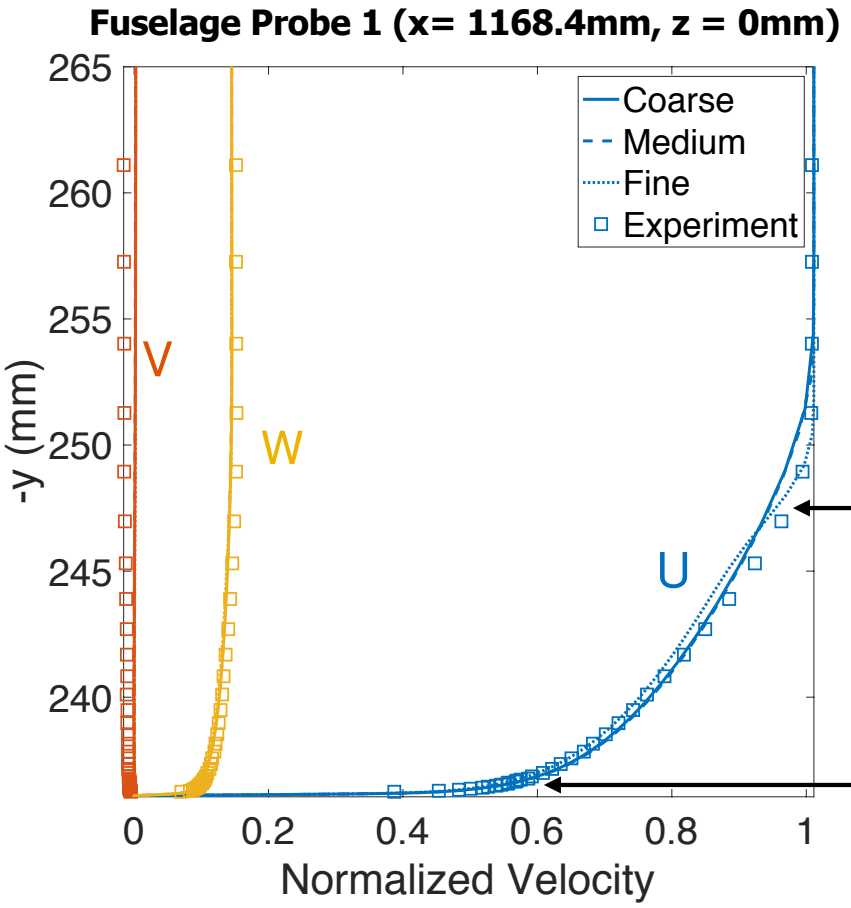
Experiment BL thickness: 20 mm

Accurate inner-layer (correct c_f predictions)

- DDES solutions on Coarse and Medium meshes are identical to RANS solutions

Fuselage probe





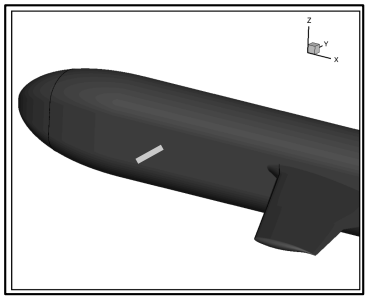
DDES (SA-RC-QCR2000)

Spurious outer-layer inflection point upon grid refinement

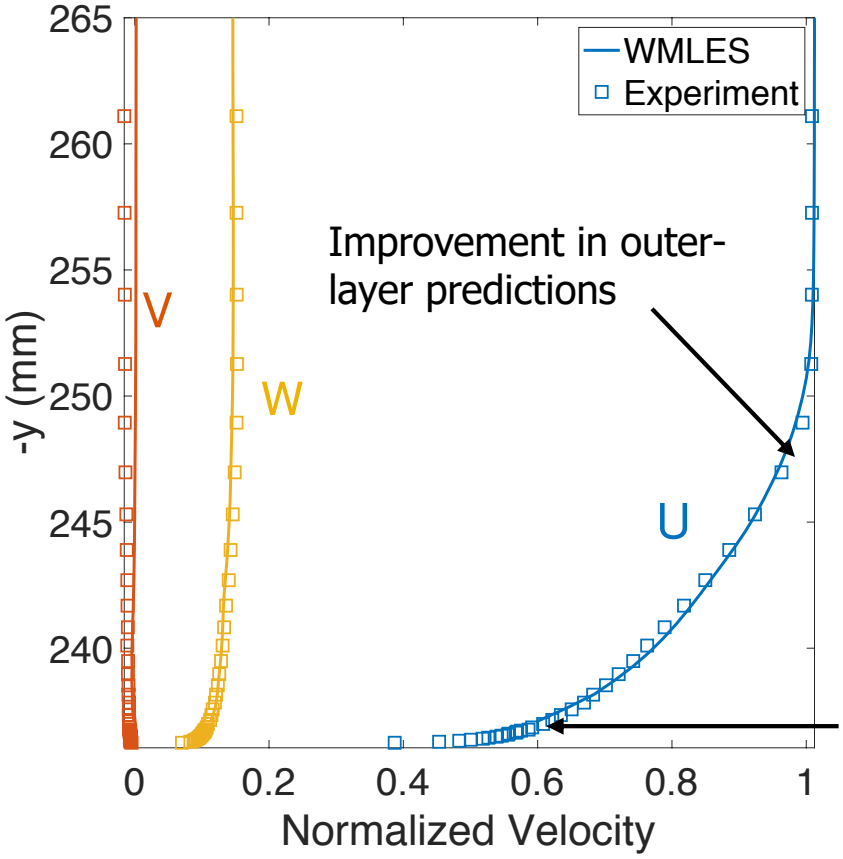
Accurate inner-layer (correct c_f predictions)

- RANS-style grid refinement leads to **deterioration of outer-layer accuracy**
- However, **no effect on c_f**
- (More on this when we consider profiles at the horn)

Fuselage probe



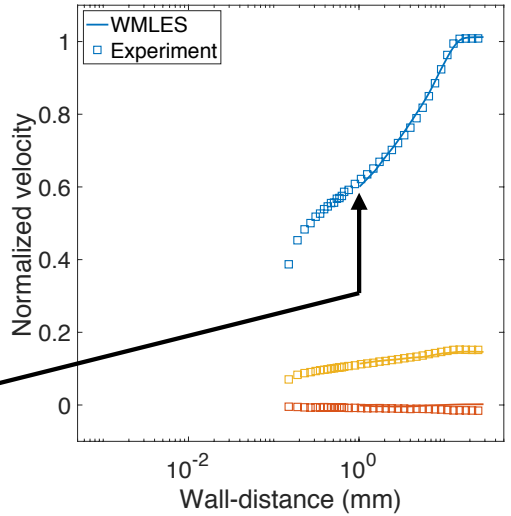
Fuselage Probe 1 (x= 1168.4mm, z = 0mm)



WMLES (Sigma SGS*, Baseline mesh)

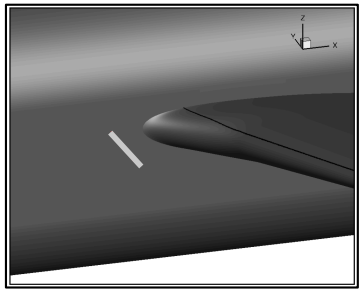
- WMLES is **tripping-aware**
- Outer-layer profile is sensitive to characterization of tripping

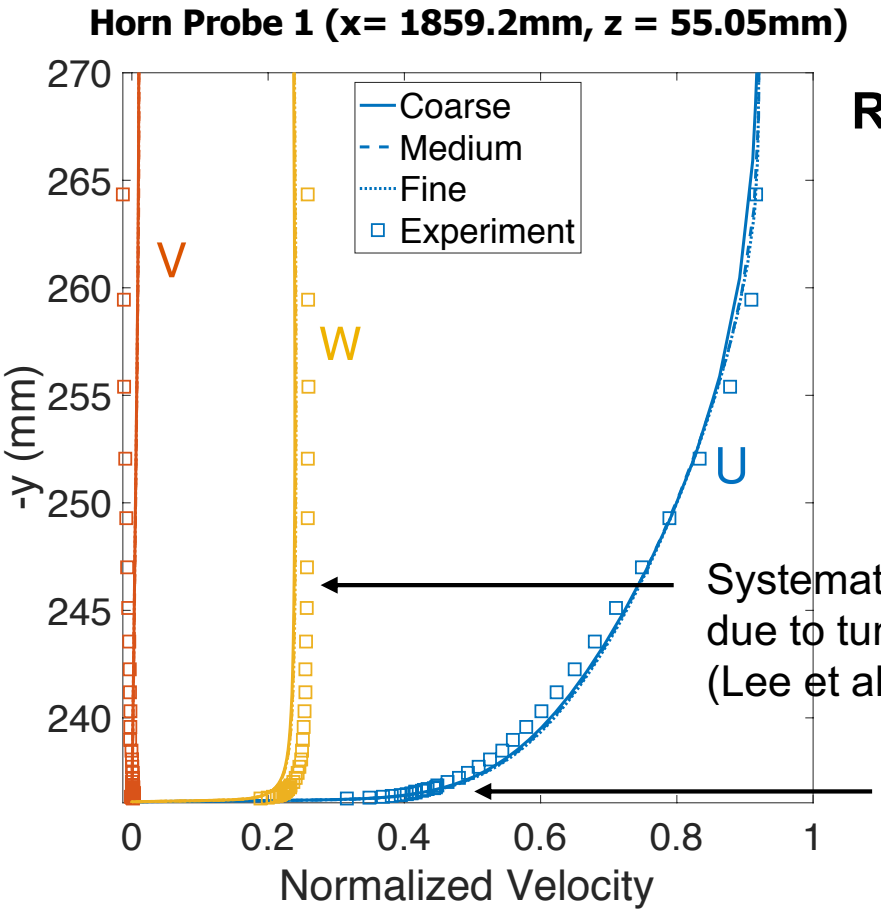
Exchange location at 1mm from wall leads to accurate c_f predictions



Nicoud et al., PoF (2011)

Horn Probe





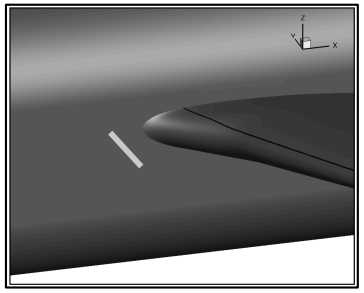
RANS (SA-RC-QCR2020)

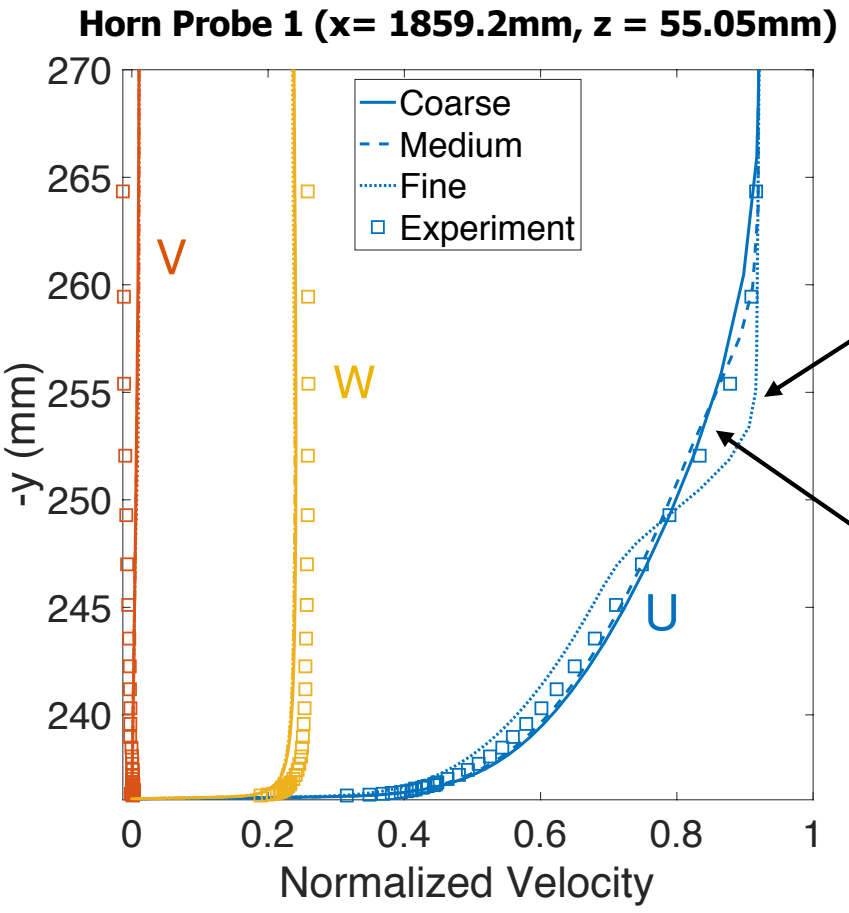
- BL thickness grown to about 25-30mm
- RANS shows little grid-dependency; more accurate outer layer for finer mesh
- Minor tunnel effects seen in terms of upwash

Systematic 6% error due to tunnel effects (Lee et al., AIAA, 2018)

Reasonably accurate inner-layer/c_f predictions

Horn Probe



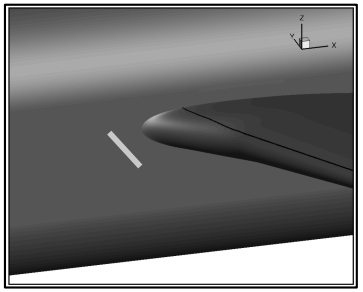


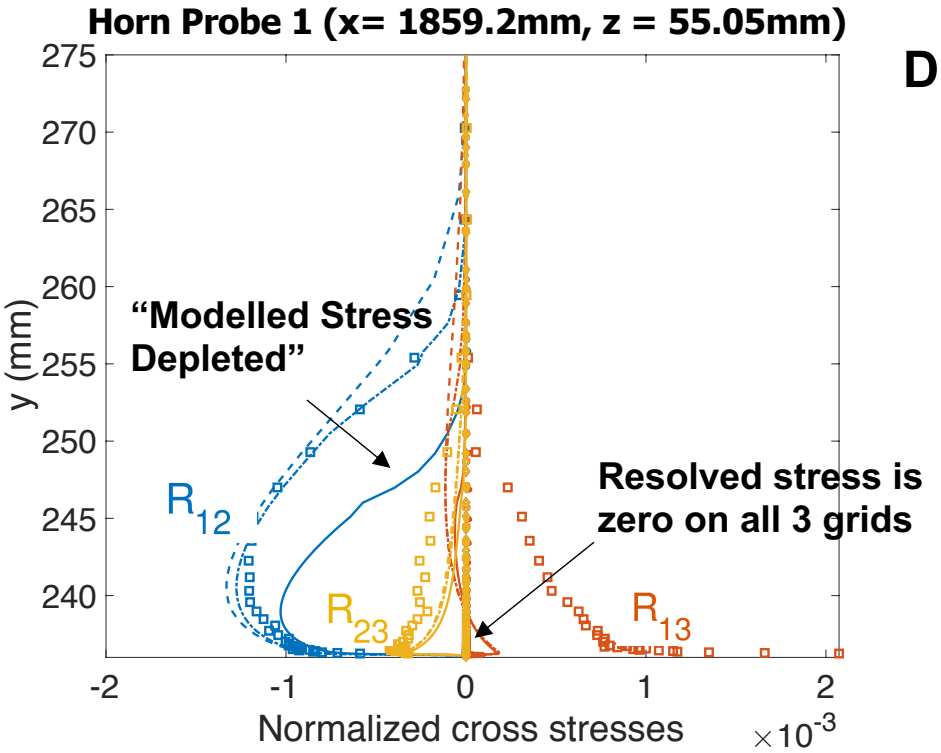
DDES (SA-RC-QCR2000)

Fine-grid solution completely deteriorated; effect seen at wall in terms of reduced c_f

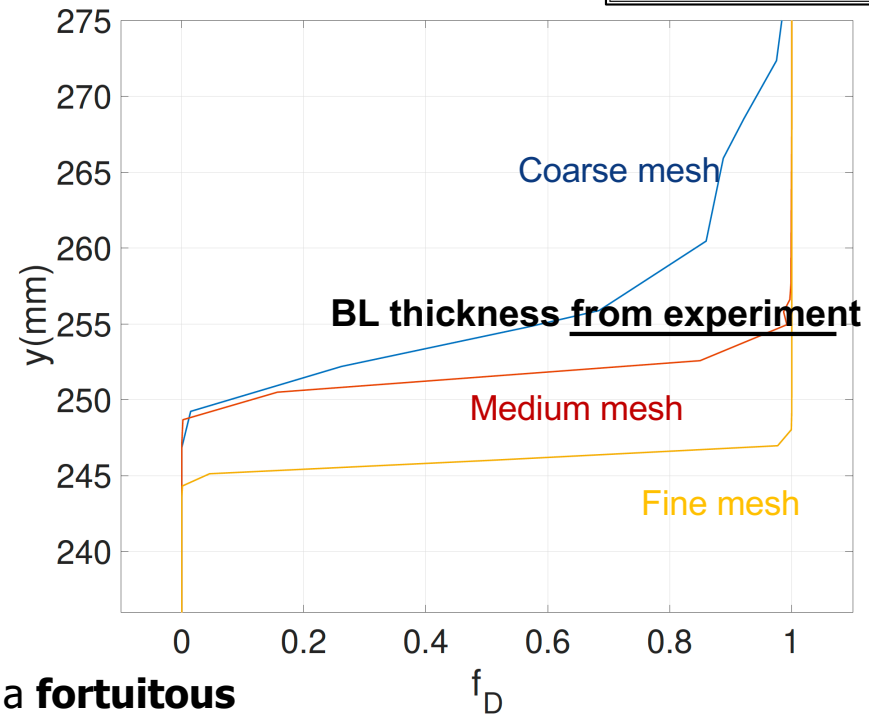
Medium-grid solution starting to show a spurious inflection; solution at wall is unaffected

Horn Probe





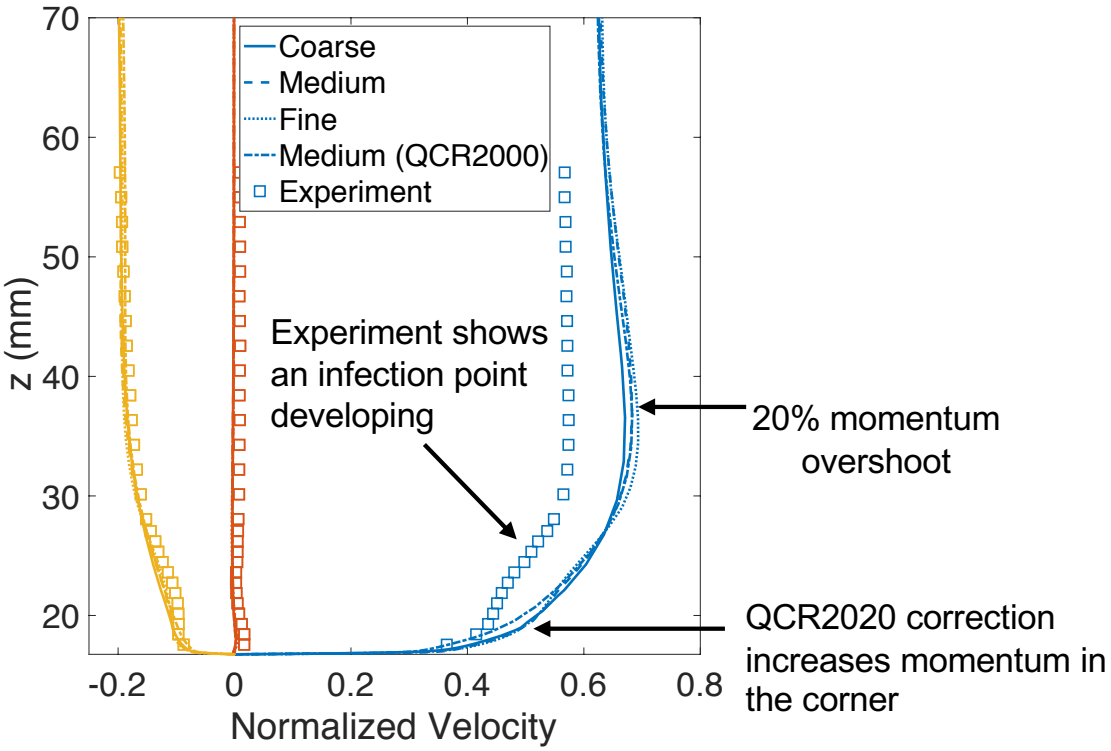
DDES (SA-RC-QCR2000)



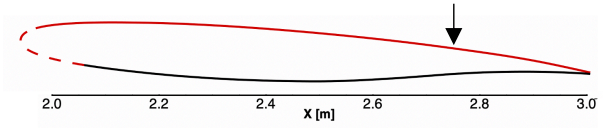
Medium mesh appears to produce "best solution" due to a **fortuitous combination** of mesh and fuselage length/wing placement!

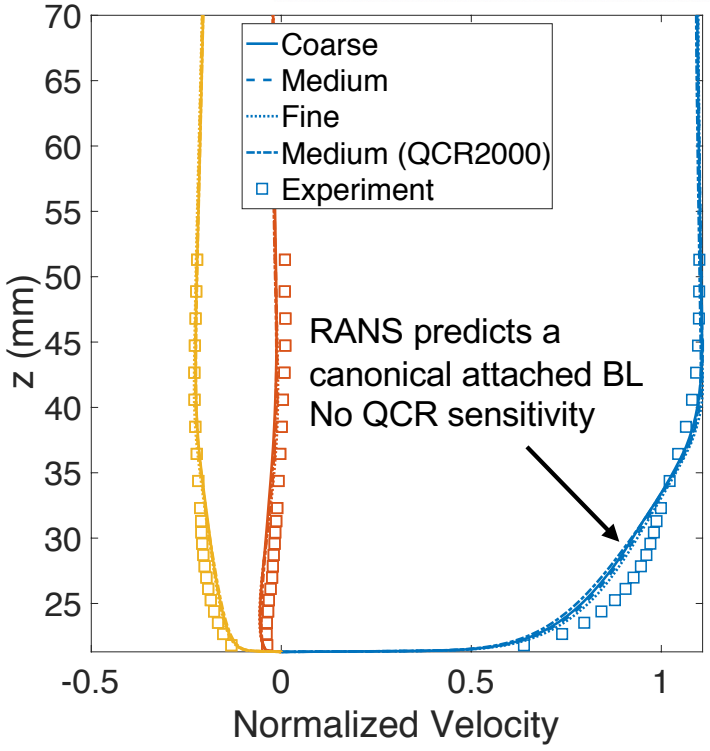
Juncture Probes at x=2747.6mm

RANS (SA-RC-QCR2020)



1mm from fuselage wall (y = -237.1mm)

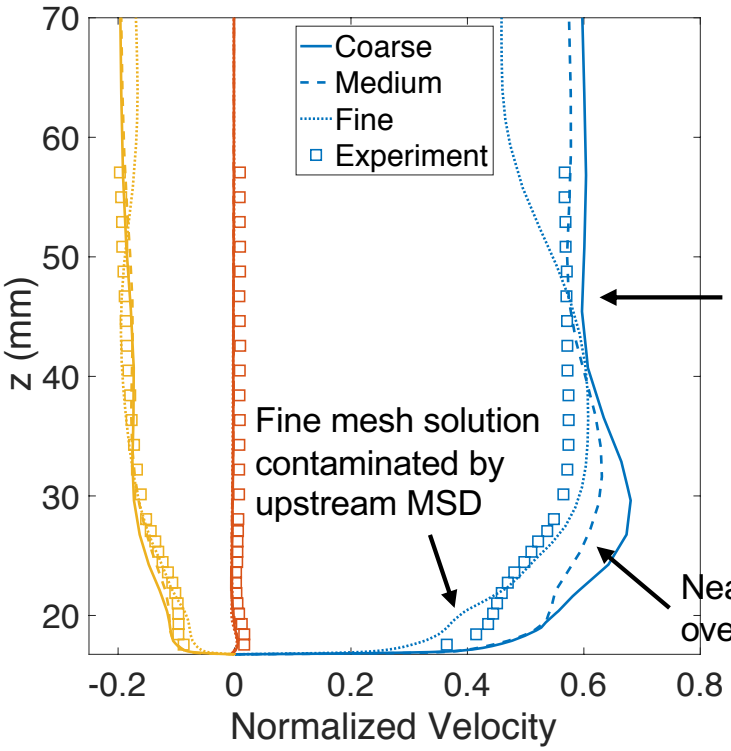




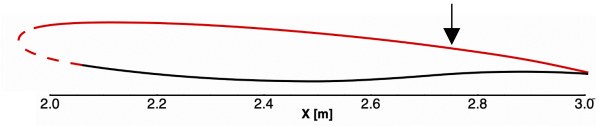
30mm from fuselage wall (y = -266.1mm)

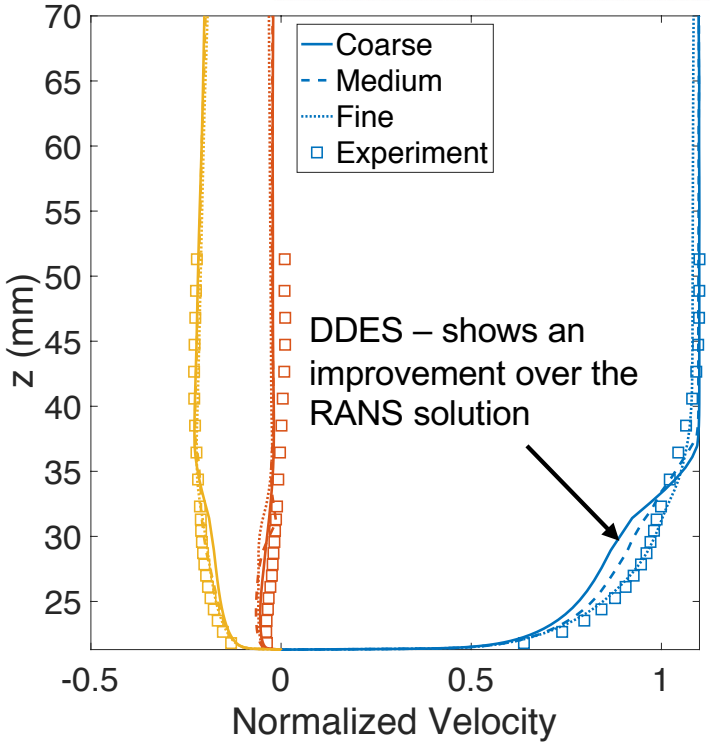
Juncture Probes at x=2747.6mm

DDES (SA-RC-QCR2000)



1mm from fuselage wall (y = -237.1mm)

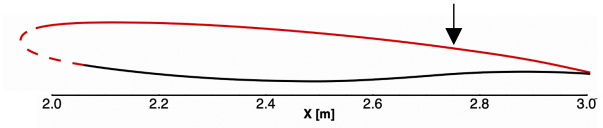


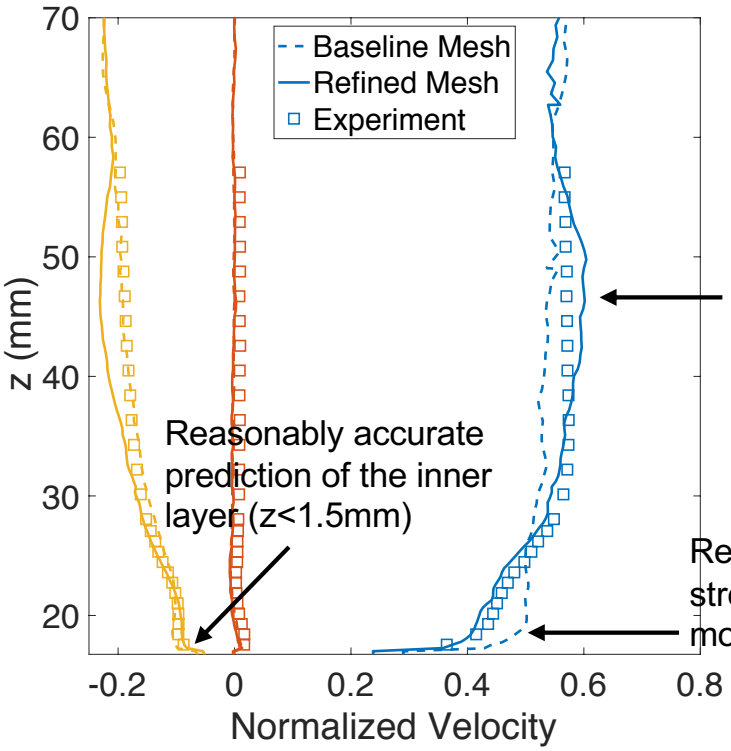


30mm from fuselage wall (y = -266.1mm)

Juncture Probes at x=2747.6mm

WMLES (Sigma SGS, exchange location=0.5mm)



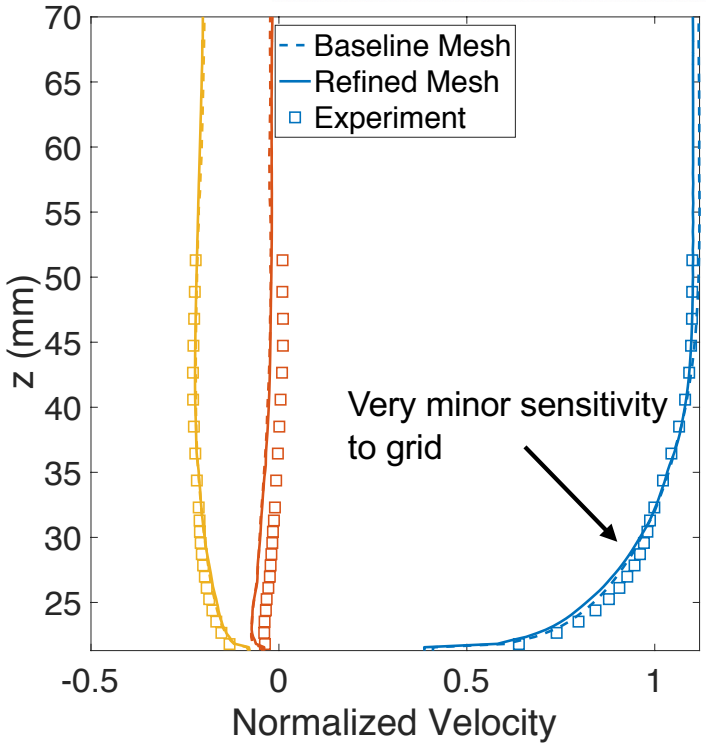


Reasonably accurate prediction of the inner layer (z<1.5mm)

Reduction in fuselage BL momentum overshoot

Reducing grid aspect ratio, streamwise spacing reduces momentum overshoot

1mm from fuselage wall (y = -237.1mm)

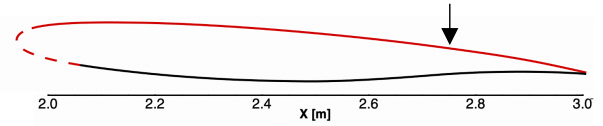


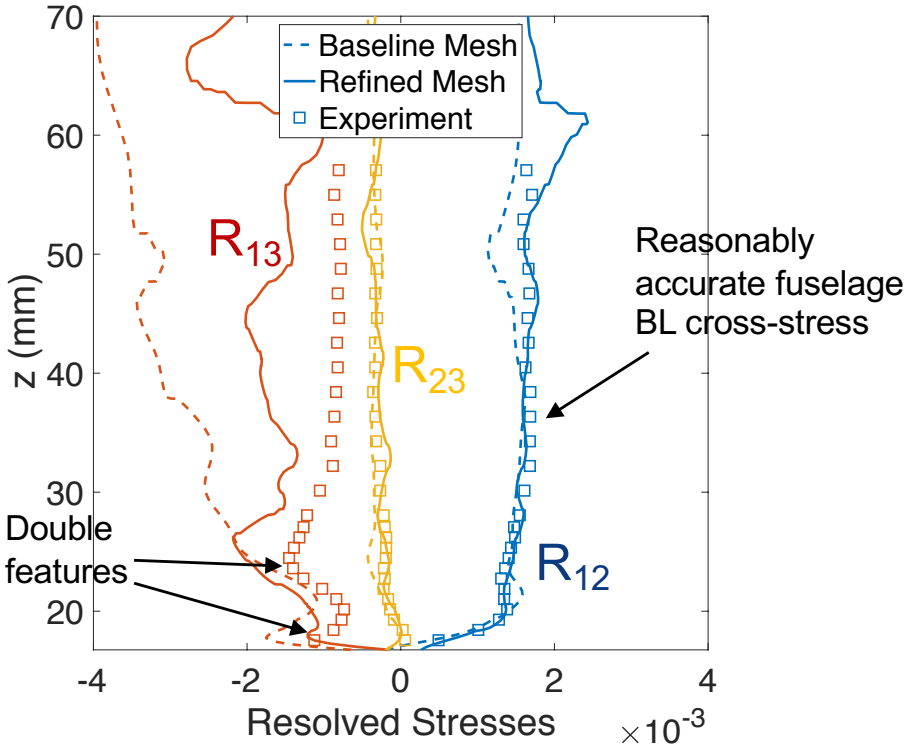
Very minor sensitivity to grid

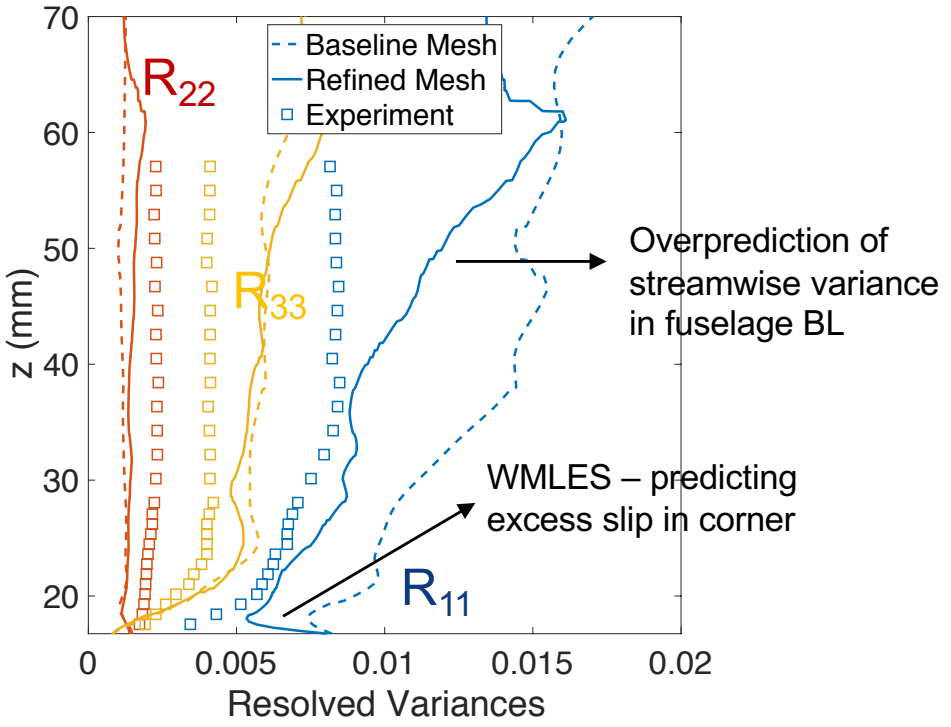
30mm from fuselage wall (y = -266.1mm)

Juncture Probes at x=2747.6mm

WMLES (Sigma SGS, exchange location=0.5mm)



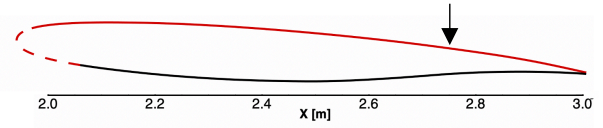


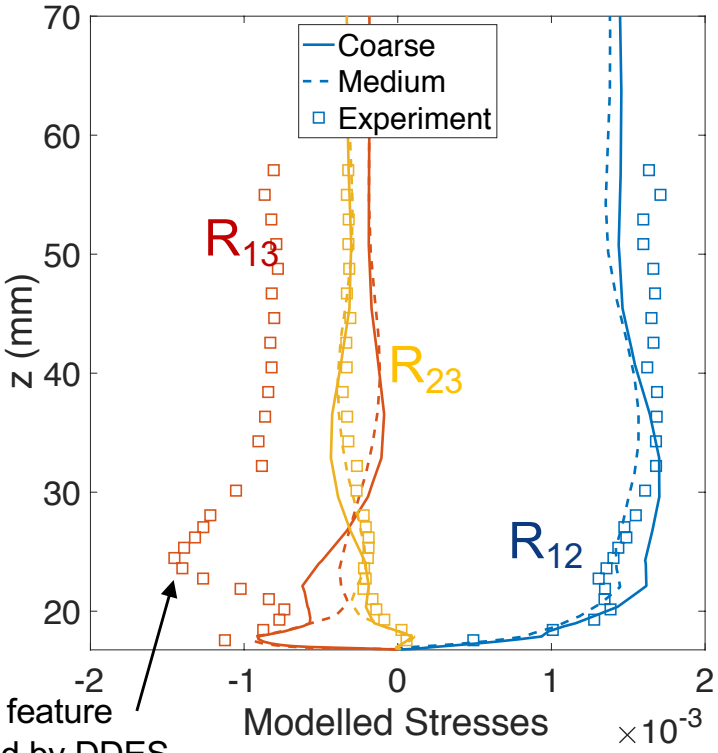


1mm from fuselage wall
(y = -237.1mm)

Juncture Probes at x=2747.6mm

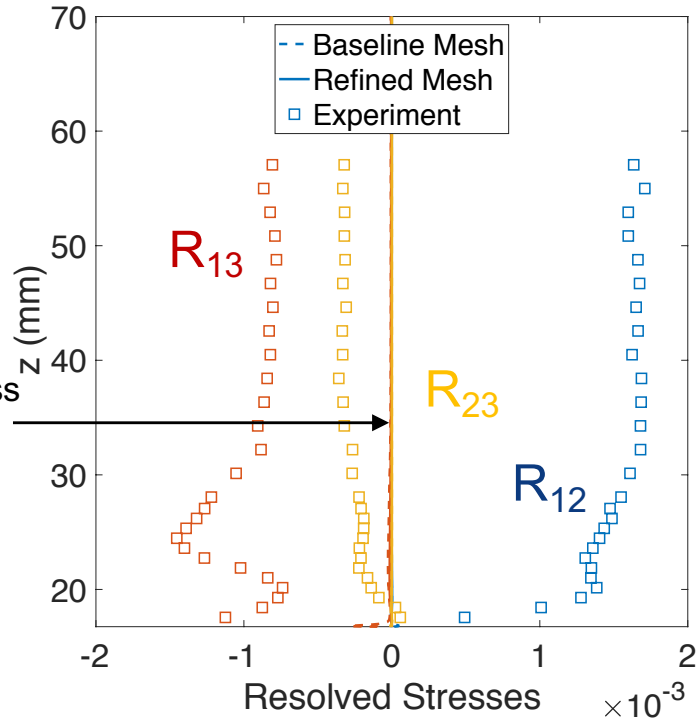
DDES (SA-RC-QCR2000)





Outer feature missed by DDES. Not resolved until post separation.

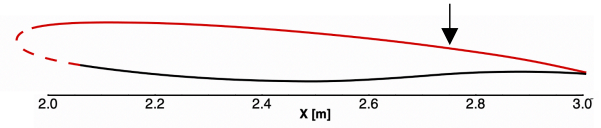
100% of stress modelled; 0% resolved



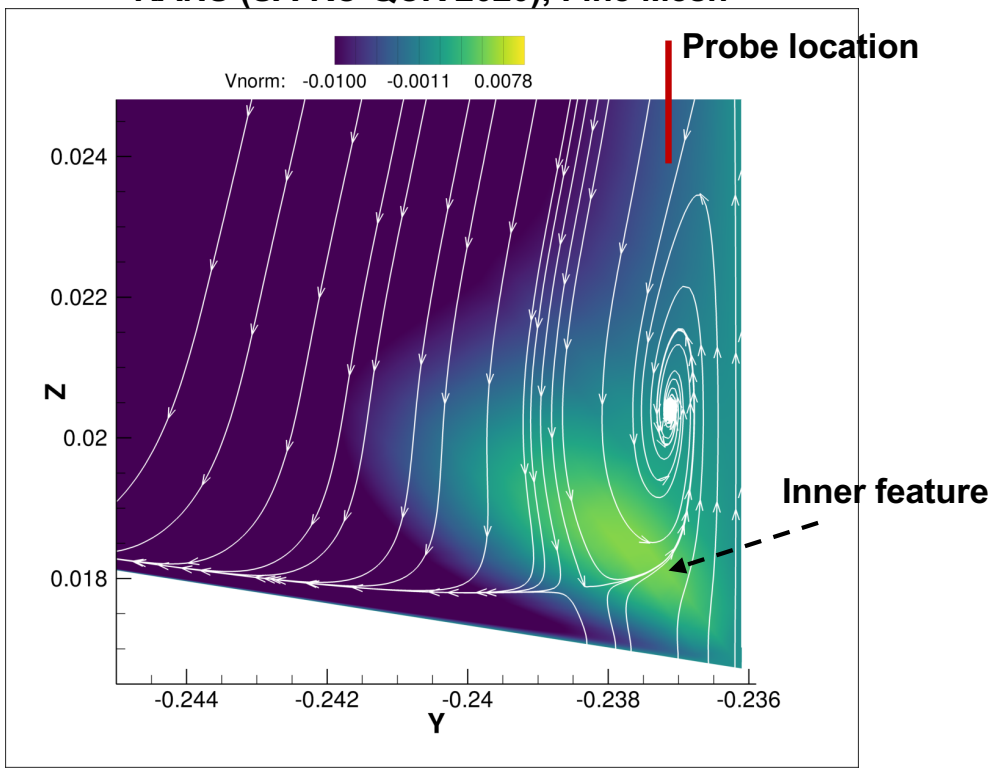
1mm from fuselage wall (y = -237.1mm)

Juncture Probes at x=2747.6mm

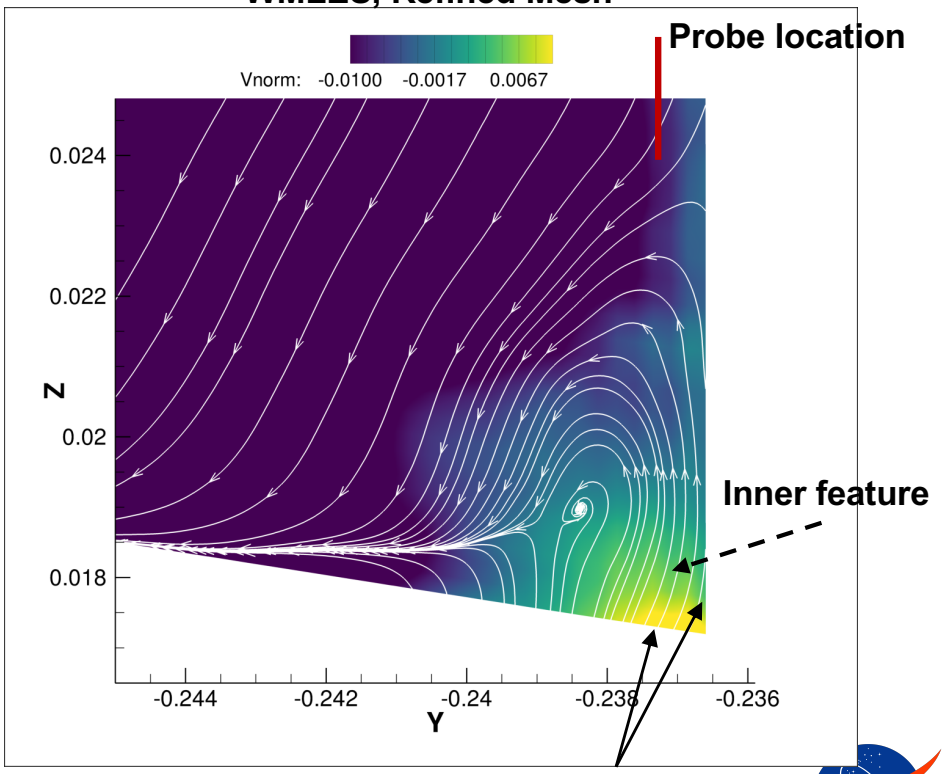
Secondary flow in the corner (Rumsey et al, 2020)



RANS (SA-RC-QCR 2020), Fine Mesh

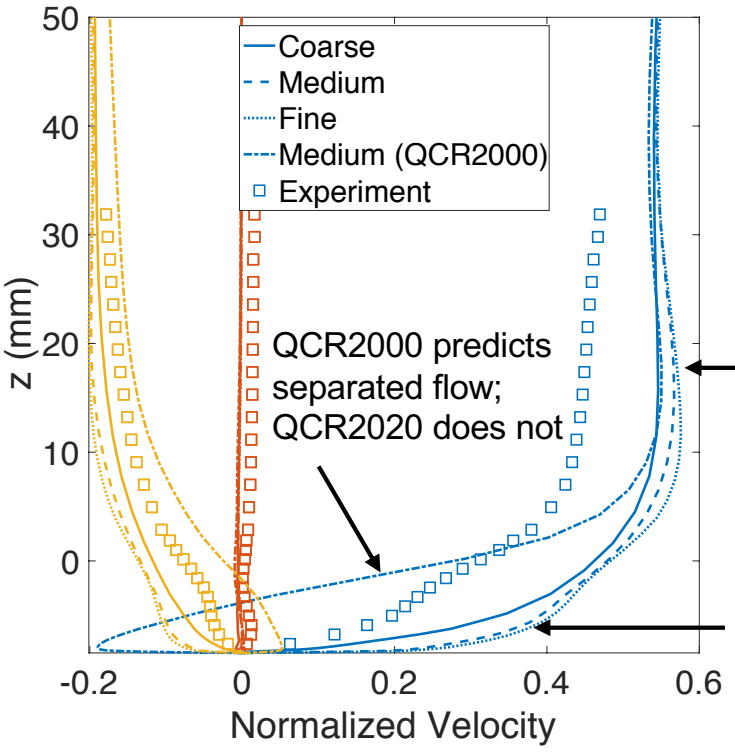


WMLES, Refined Mesh



Juncture Probes at x=2852.6mm

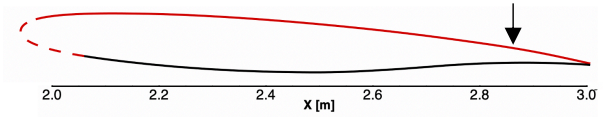
RANS (SA-RC-QCR2020)

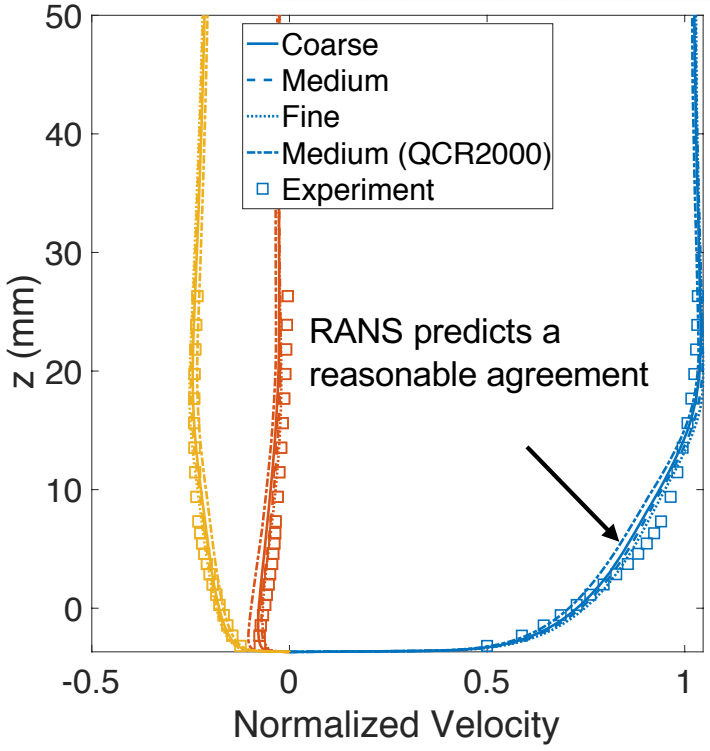


25% momentum overshoot

Momentum overshoot in the corner; grid refinement increases overshoot

1mm from fuselage wall (y = -237.1mm)

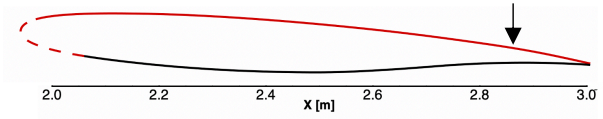


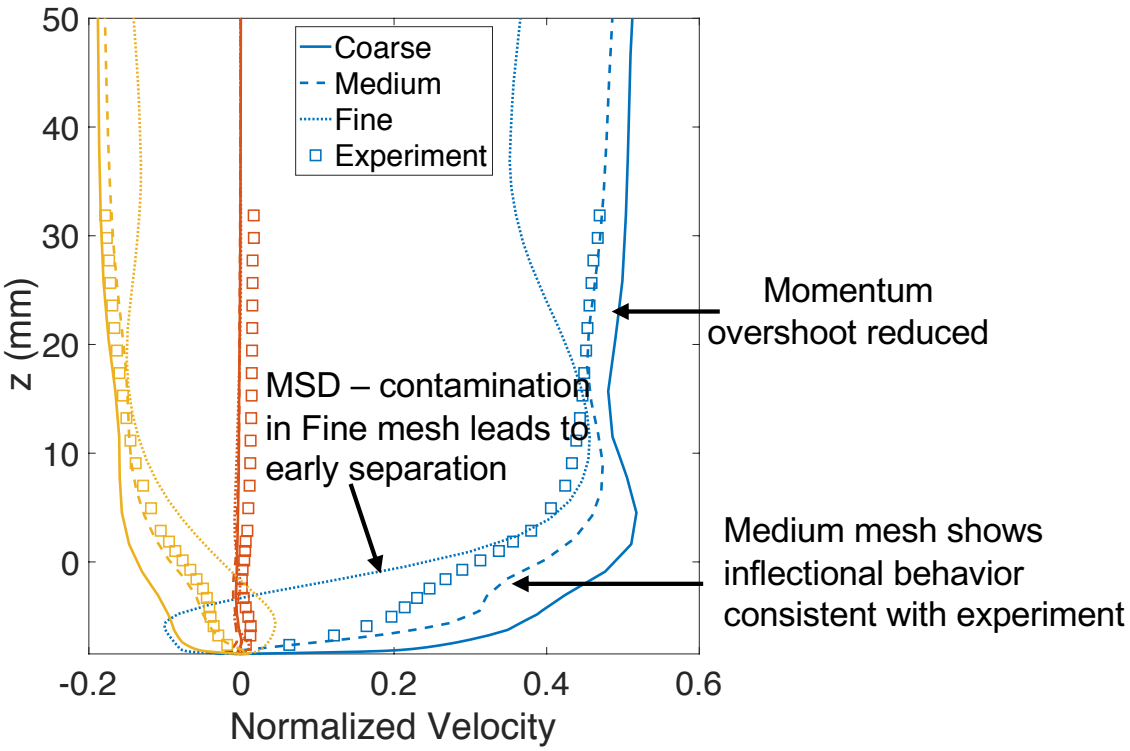


30mm from fuselage wall (y = -266.1mm)

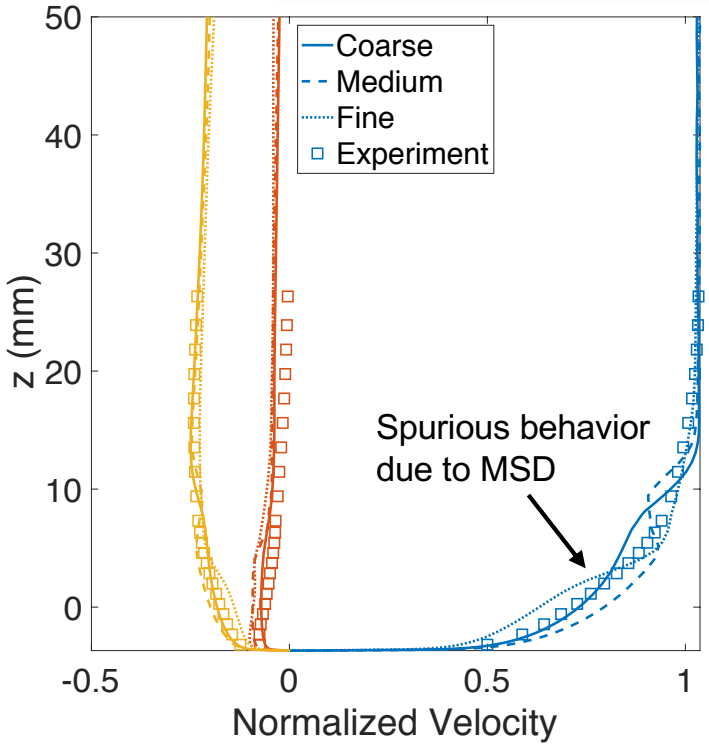
Juncture Probes at x=2852.6mm

DDES (SA-RC-QCR2000): Mesh resolution





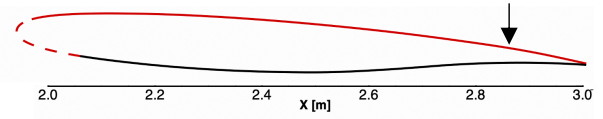
1mm from fuselage wall
(y = -237.1mm)

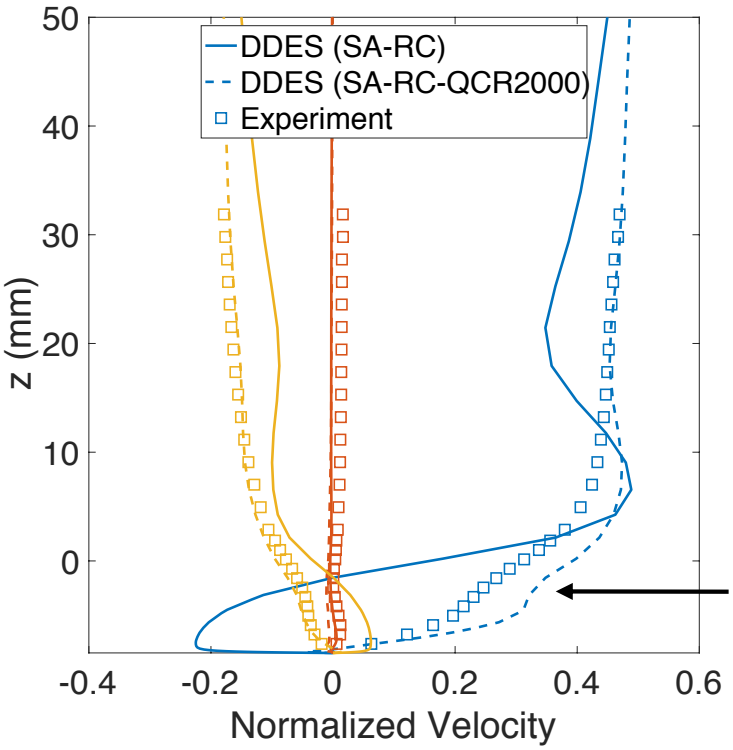


30mm from fuselage wall
(y = -266.1mm)

Juncture Probes at x=2852.6mm

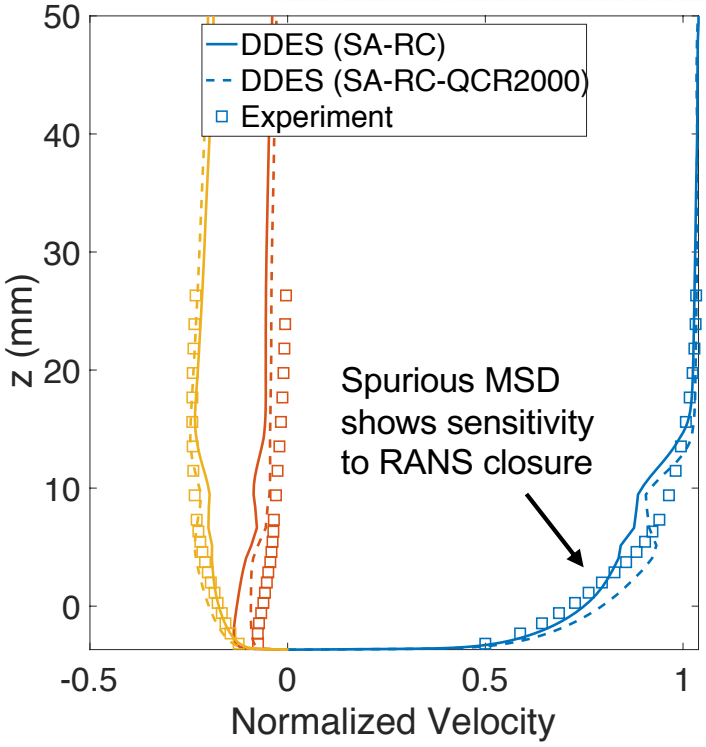
DDES (SA-RC-QCR2000): Underlying RANS closure





1mm from fuselage wall
(y = -237.1mm)

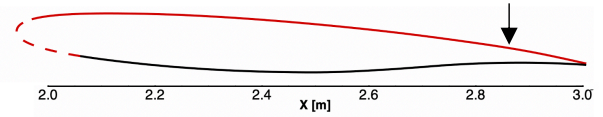
QCR-2000 correction underlying RANS closure improves early onset prediction for uncorrected closure

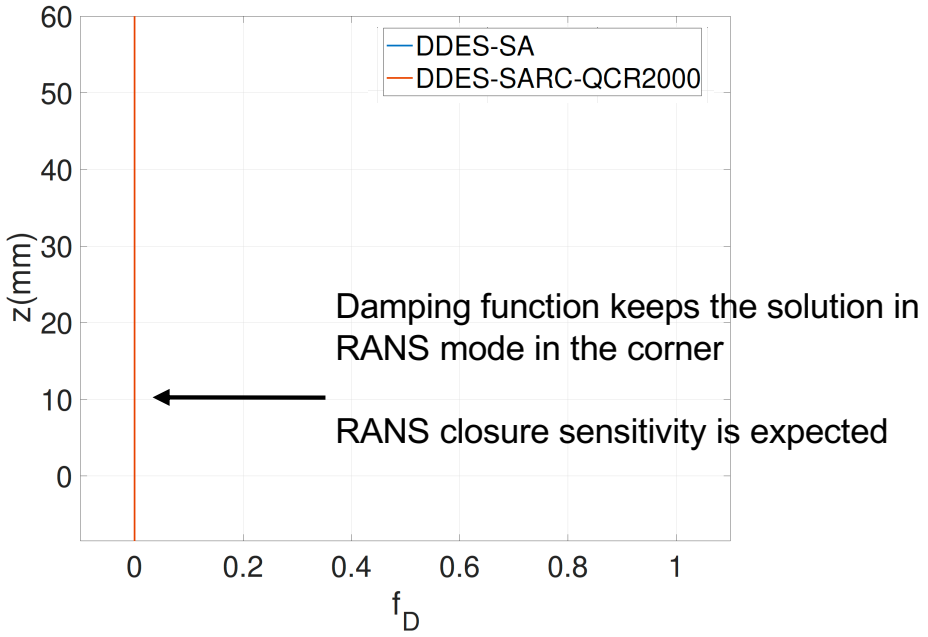


30mm from fuselage wall
(y = -266.1mm)

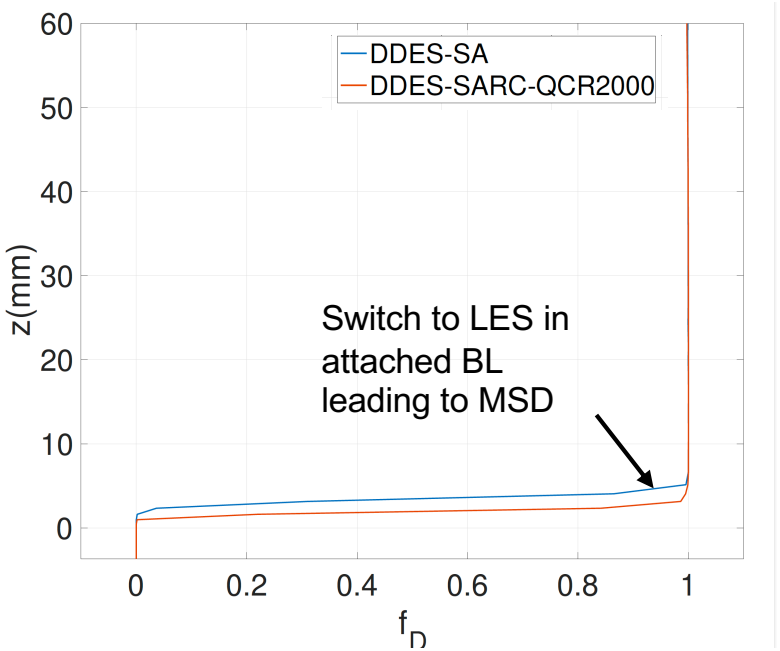
Juncture Probes at x=2852.6mm

DDES (SA-RC-QCR2000): Underlying RANS closure





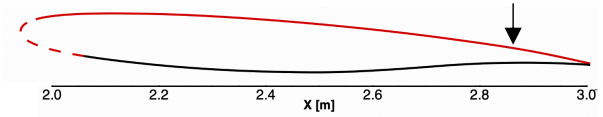
1mm from fuselage wall
(y = -237.1mm)

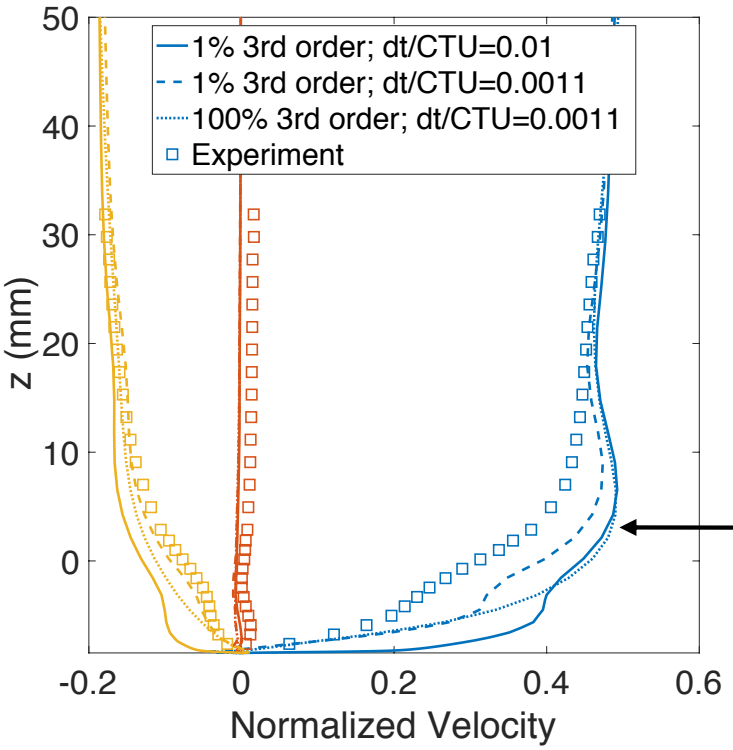


30mm from fuselage wall
(y = -266.1mm)

Juncture Probes at x=2852.6mm

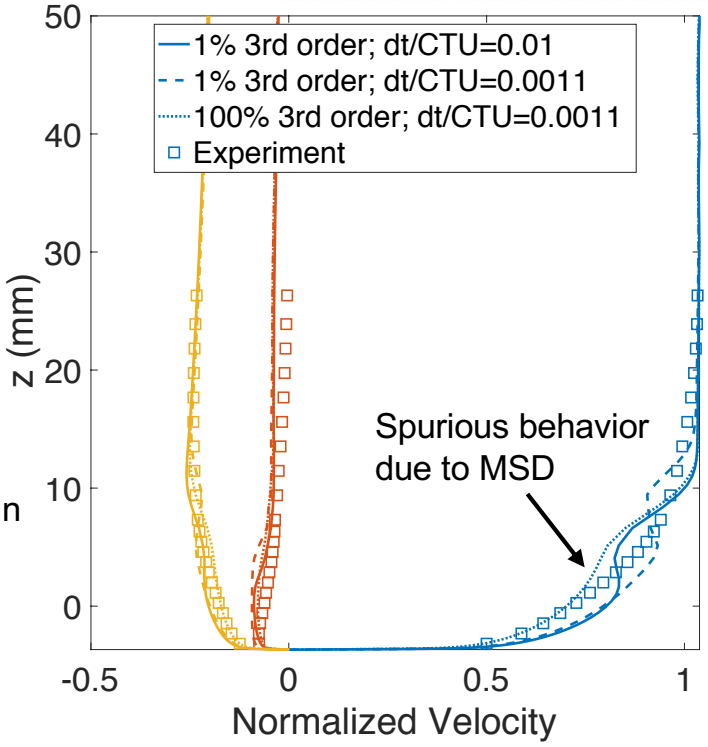
DDES (SA-RC-QCR2000): Numerical dissipation





1mm from fuselage wall
(y = -237.1mm)

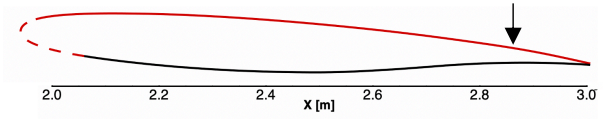
Maximum overshoot in dissipative numerics

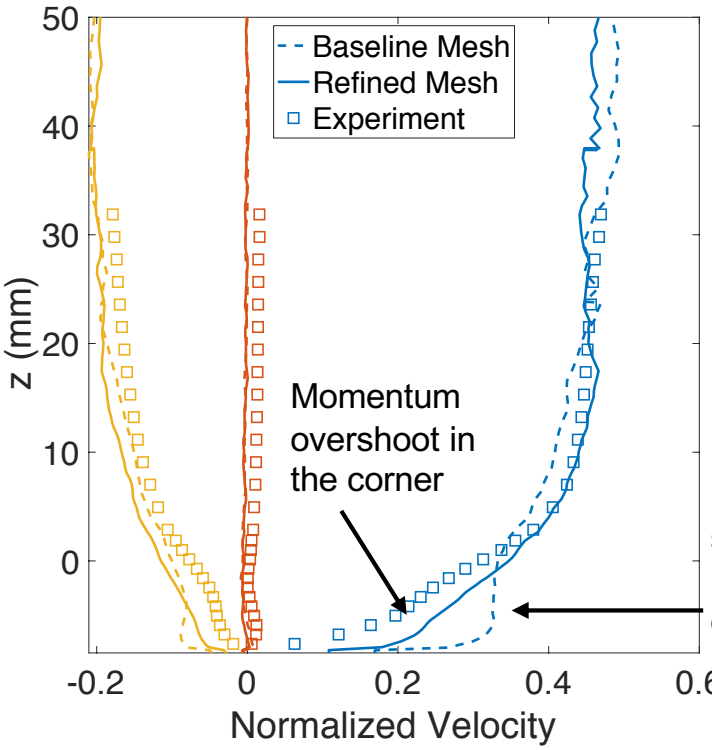


30mm from fuselage wall
(y = -266.1mm)

Juncture Probes at x=2852.6mm

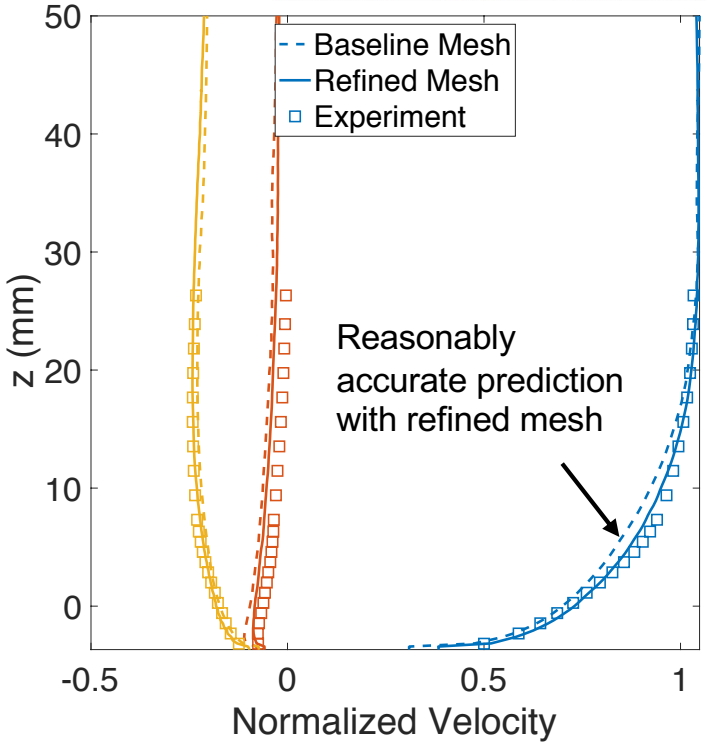
WMLES (Sigma SGS, exchange location=0.5mm)





Improvement to streamwise spacing reduces momentum overshoot

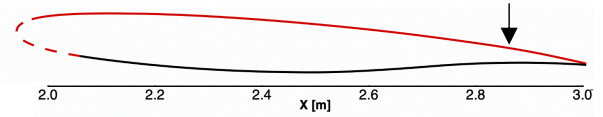
1mm from fuselage wall (y = -237.1mm)

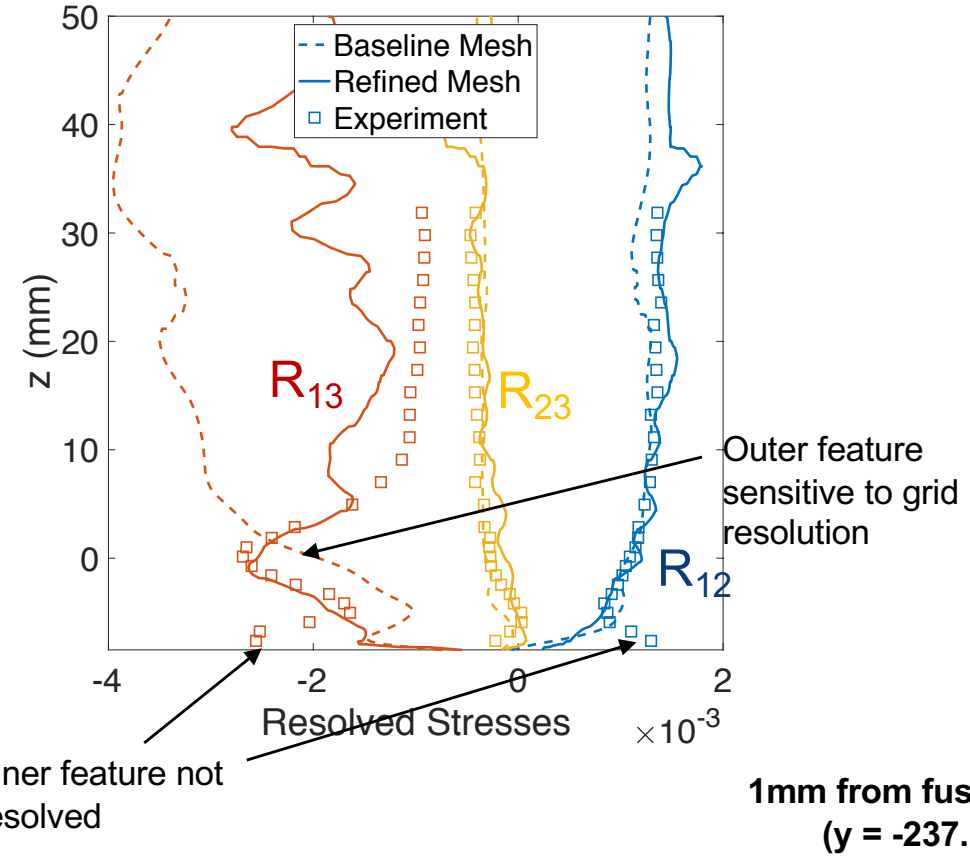


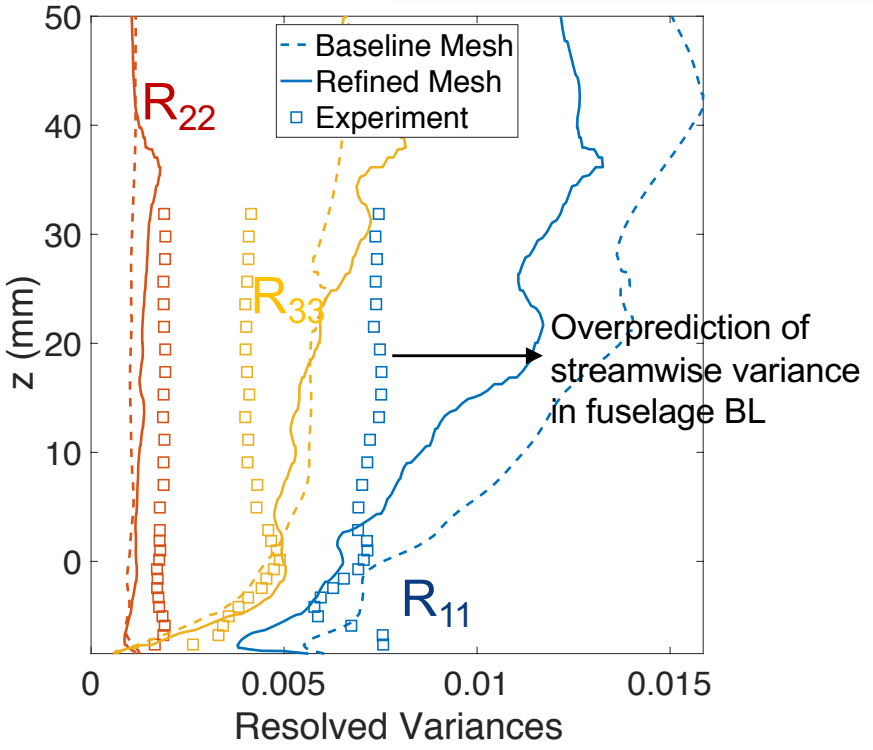
30mm from fuselage wall (y = -266.1mm)

Juncture Probes at x=2852.6mm

WMLES (Sigma SGS, exchange location=0.5mm)



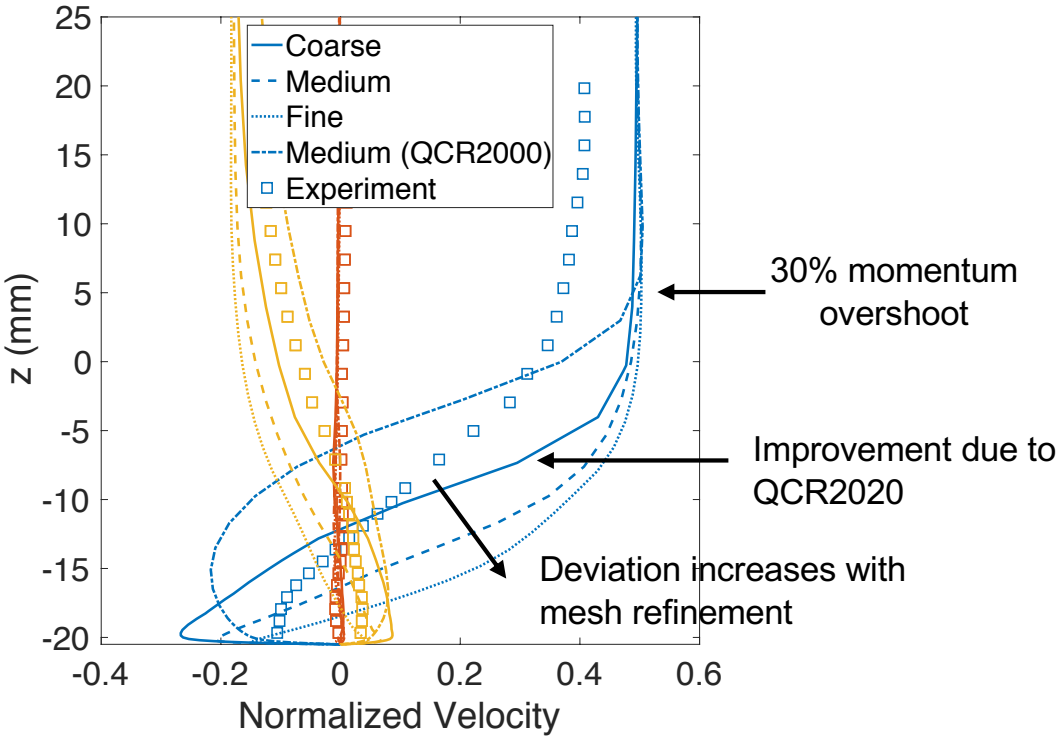




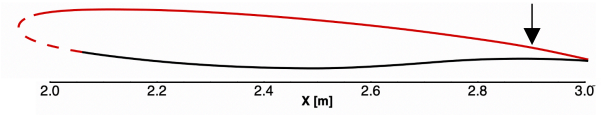
1mm from fuselage wall (y = -237.1mm)

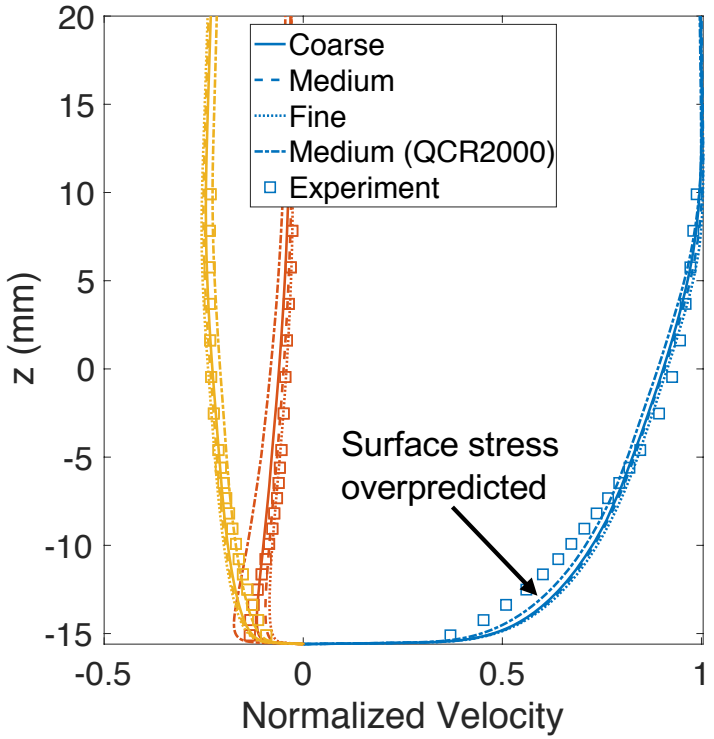
Juncture Probes at x=2892.6mm

RANS (SA-RC-QCR2020)



1mm from fuselage wall (y = -237.1mm)

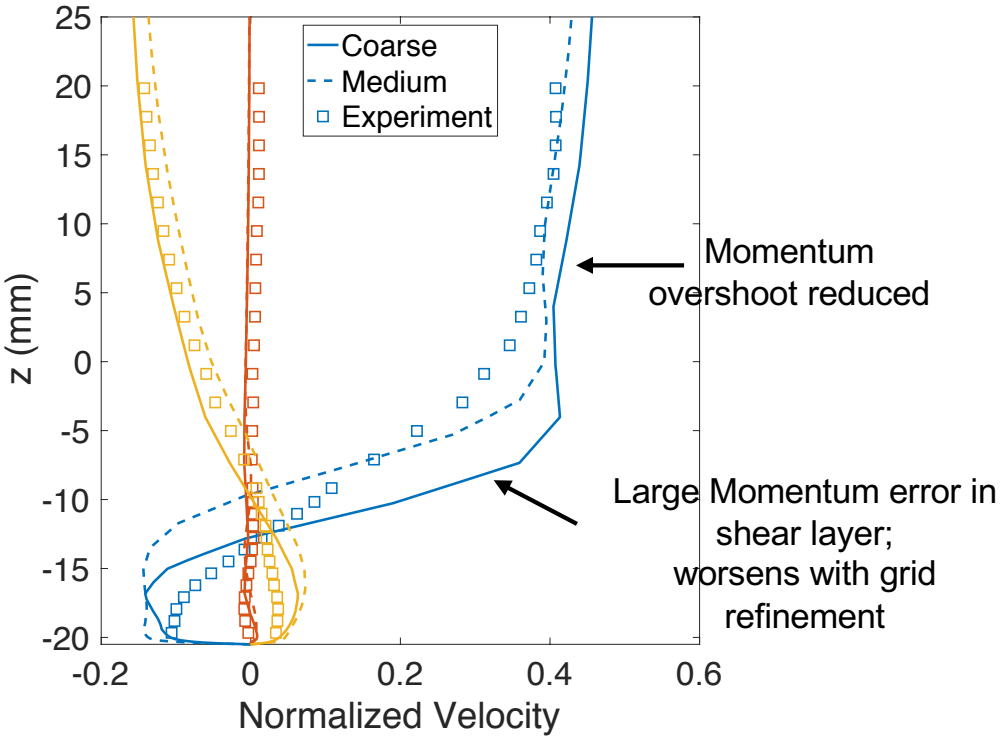




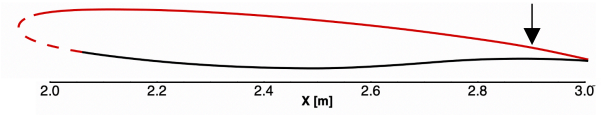
30mm from fuselage wall (y = -266.1mm)

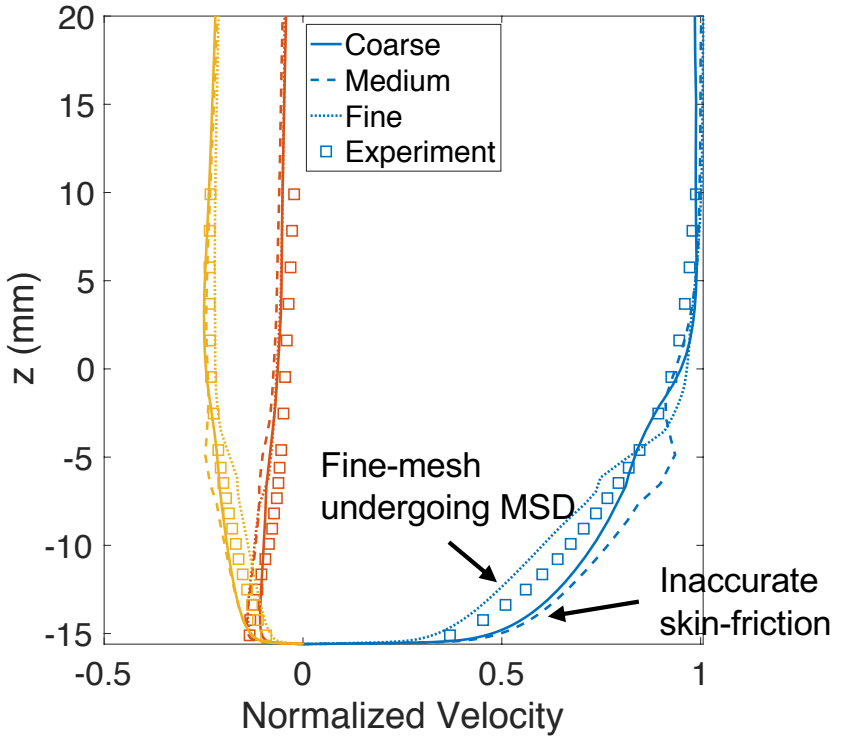
Juncture Probes at x=2892.6mm

DDES (SA-RC-QCR2000)



1mm from fuselage wall (y = -237.1mm)

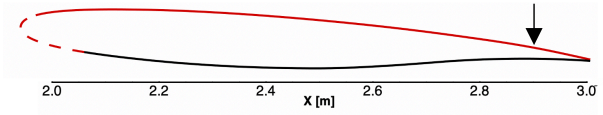


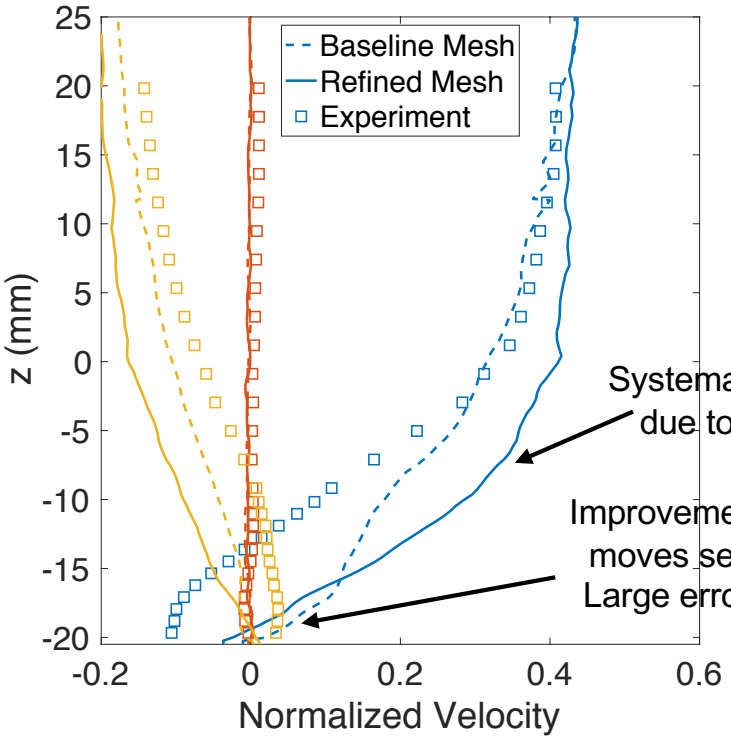


30mm from fuselage wall (y = -266.1mm)

Juncture Probes at x=2892.6mm

WMLES (Sigma SGS, exchange location=0.5mm)

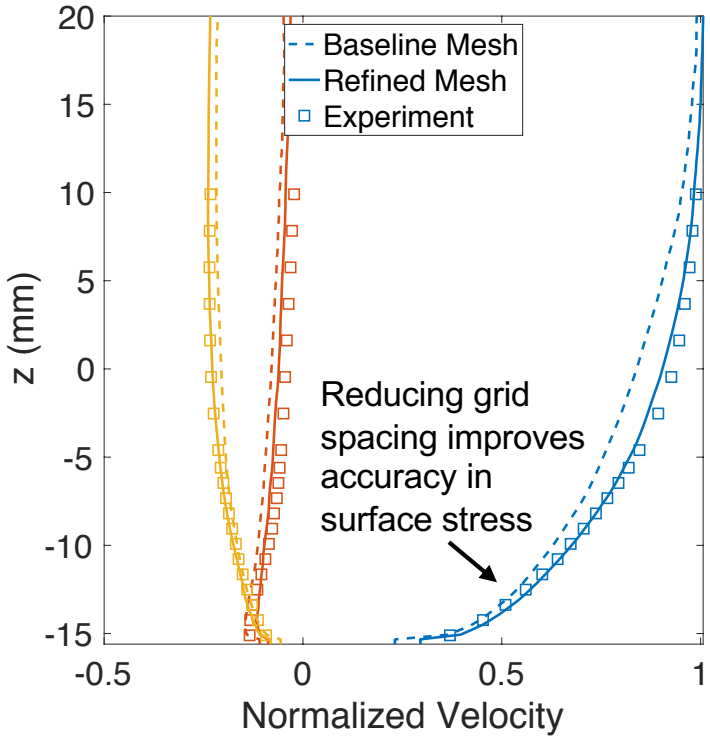




Systematic shift in momentum due to delayed separation

Improvement in streamwise spacing moves separation point upstream
Large error on onset of separation

1mm from fuselage wall (y = -237.1mm)

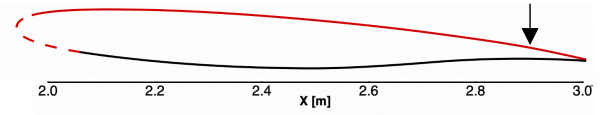


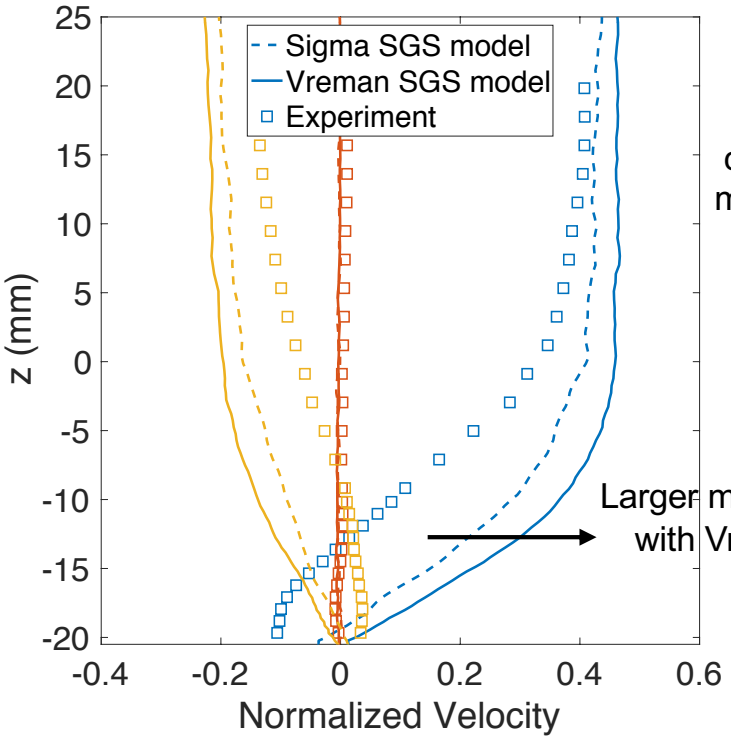
Reducing grid spacing improves accuracy in surface stress

30mm from fuselage wall (y = -266.1mm)

Juncture Probes at x=2892.6mm

WMLES (SGS sensitivity, exchange location=0.5mm)



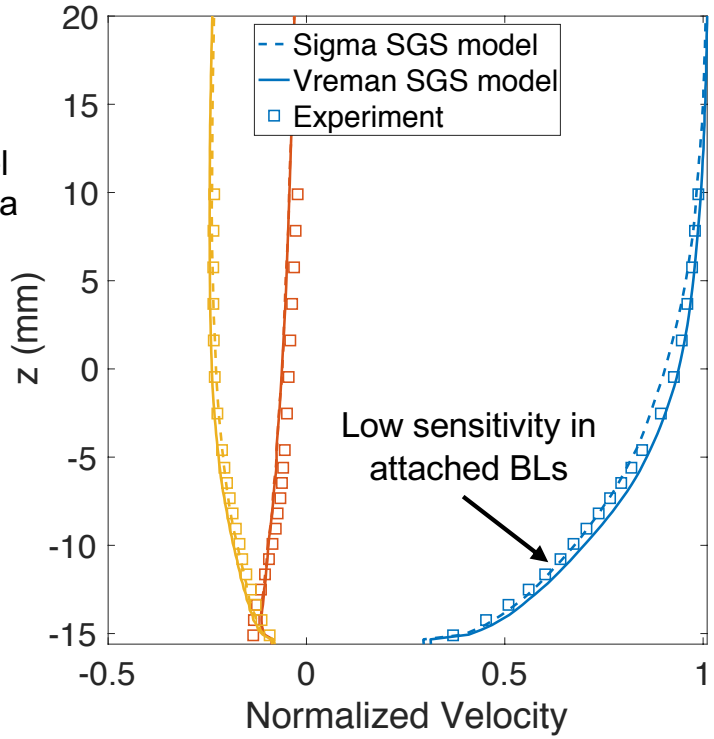


1mm from fuselage wall (y = -237.1mm)

For the choice of fixed coefficients, Vreman model more dissipative than Sigma SGS model

Larger momentum error with Vreman model

Solution likely to be sensitive to choice of model constant

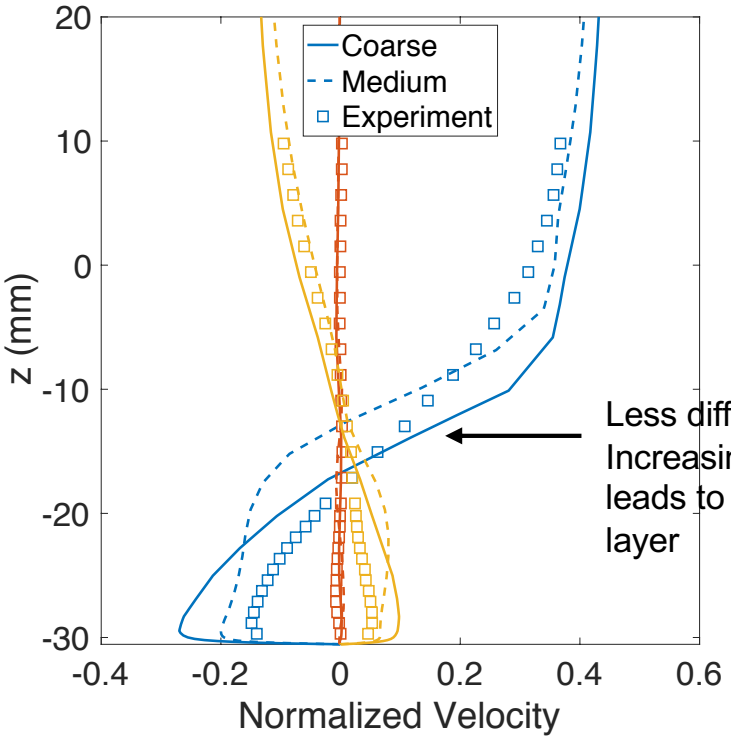


30mm from fuselage wall (y = -266.1mm)

Vreman, PoF (2004)

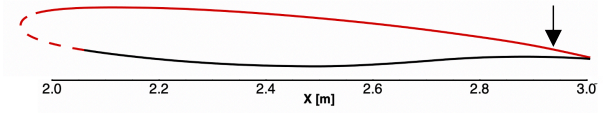
Juncture Probes at x=2922.6mm

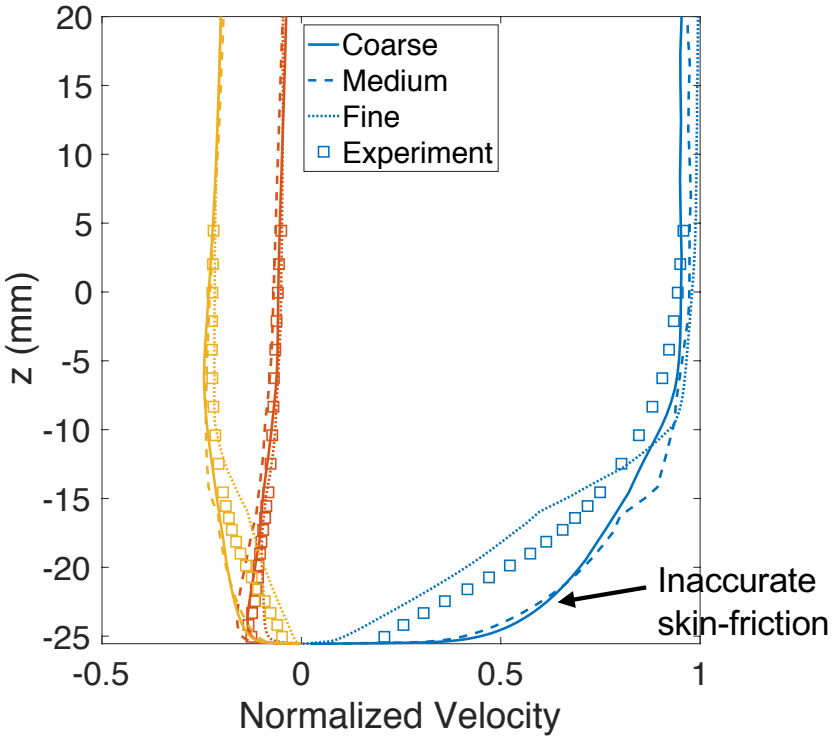
DDES (SA-RC-QCR2000)



Less diffused shear layer. Increasing grid-resolution leads to more diffused shear layer

1mm from fuselage wall (y = -237.1mm)



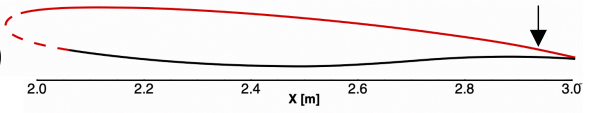


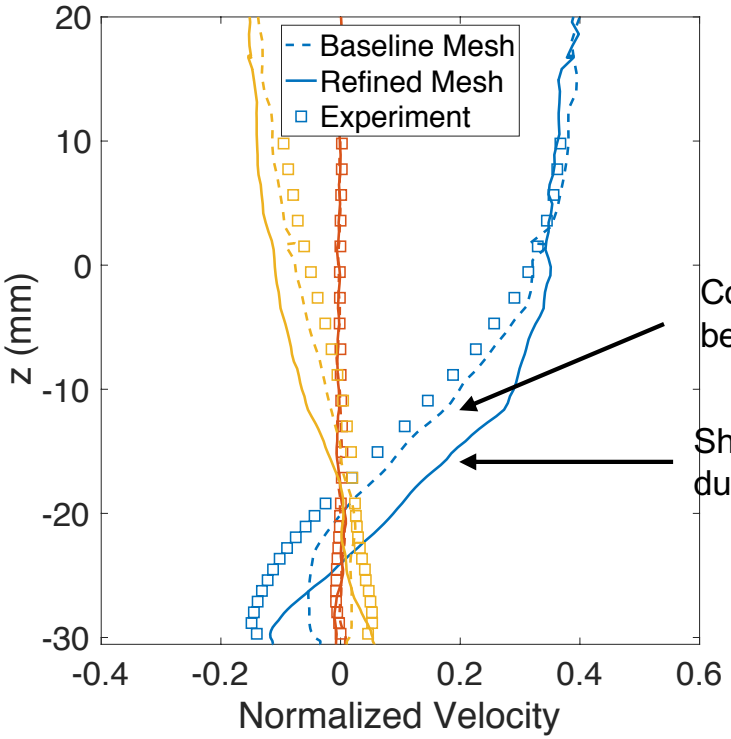
Inaccurate skin-friction

30mm from fuselage wall (y = -266.1mm)

Juncture Probes at x=2922.6mm

WMLES (Sigma SGS model, exchange location=0.5mm)

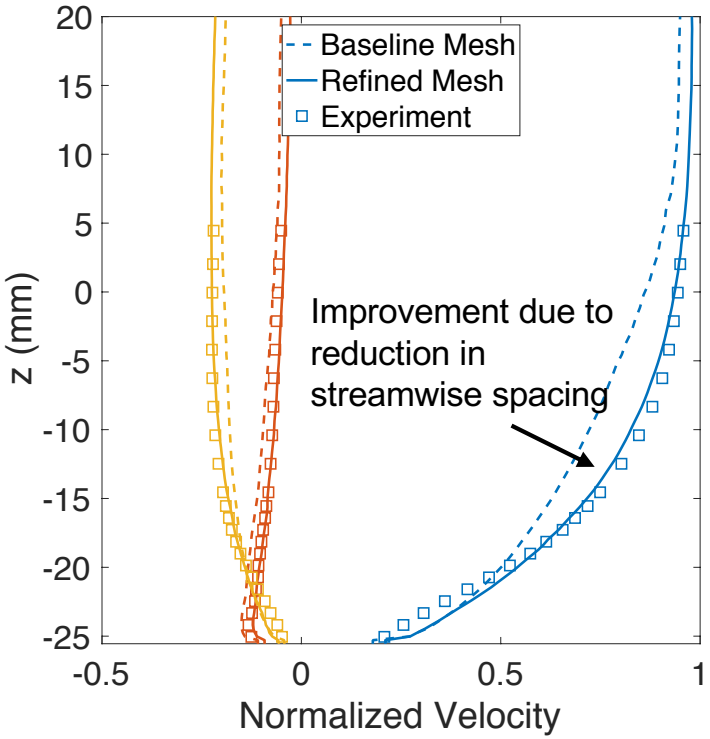




Coarser mesh does better? Fortuitous?

Shift in shear layer due to delayed onset

1mm from fuselage wall (y = -237.1mm)

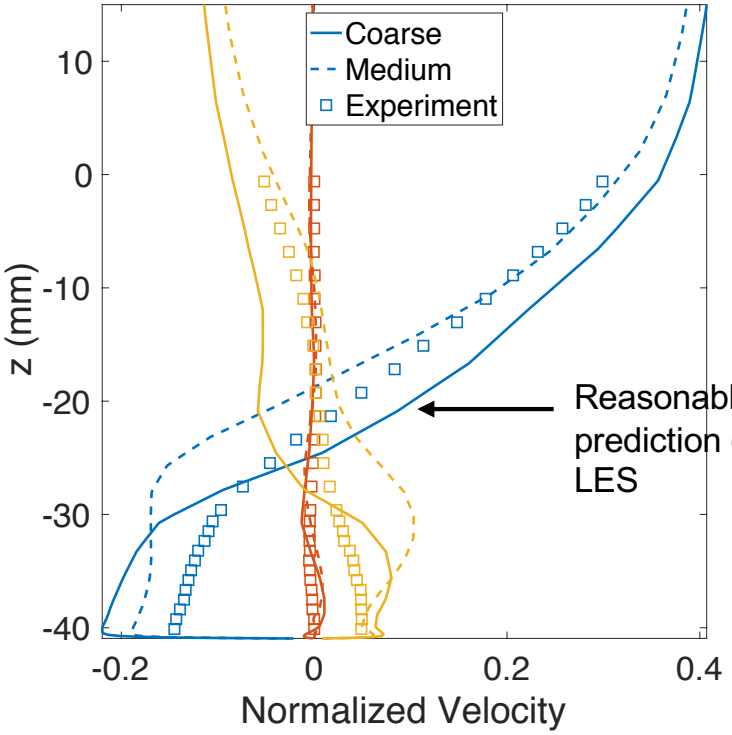


Improvement due to reduction in streamwise spacing

30mm from fuselage wall (y = -266.1mm)

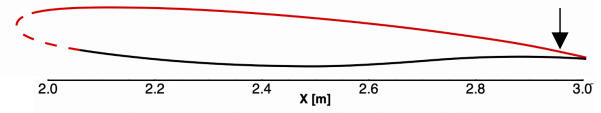
Juncture Probes at x=2952.6mm

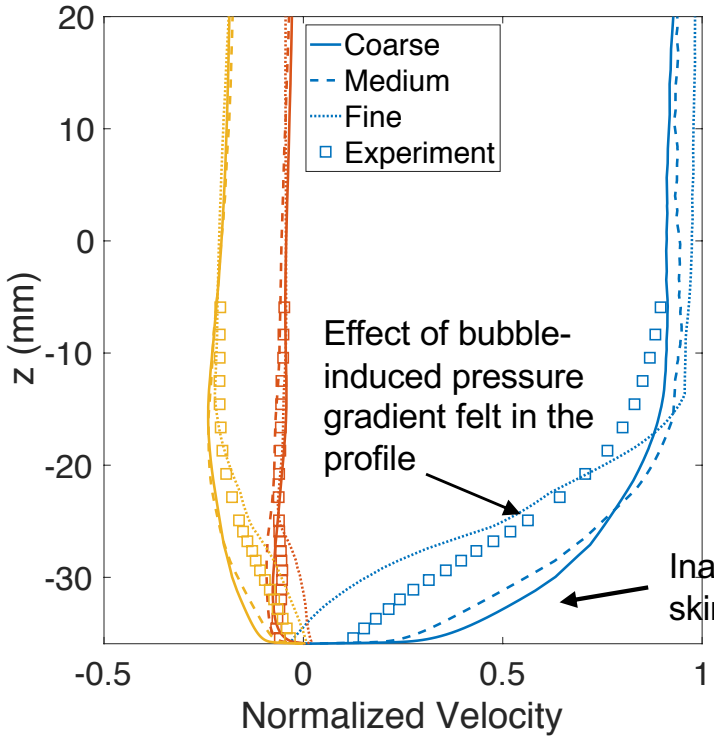
DDES (SA-RC-QCR2000)



Reasonably accurate prediction due to switch to LES

1mm from fuselage wall (y = -237.1mm)





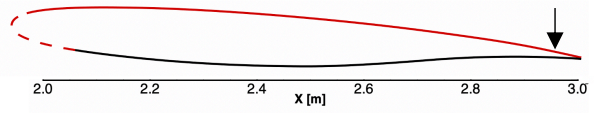
Effect of bubble-induced pressure gradient felt in the profile

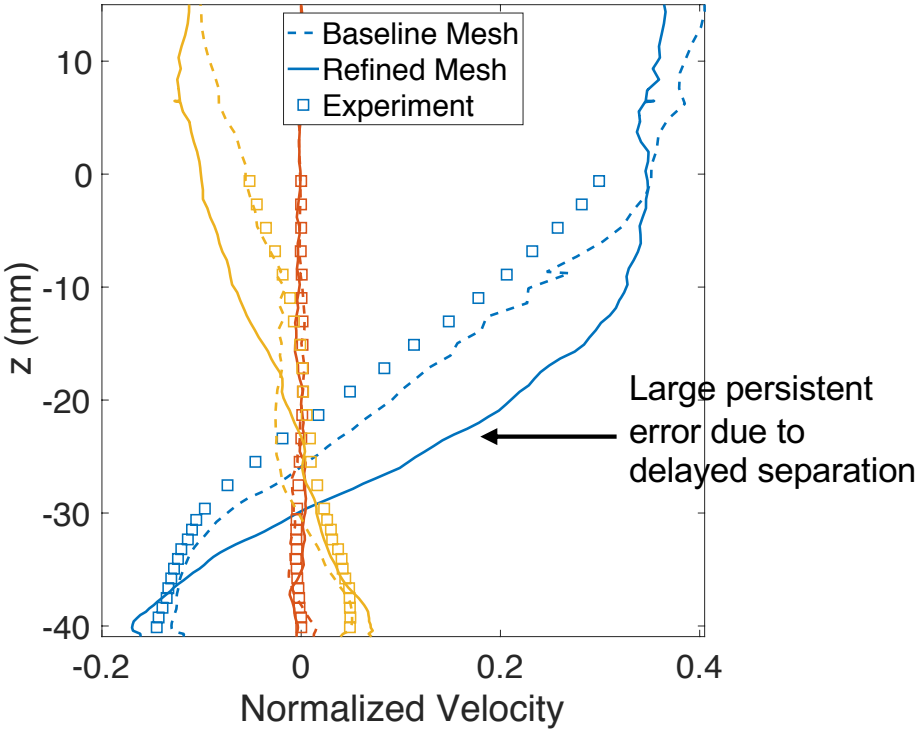
Inaccurate skin-friction

30mm from fuselage wall (y = -266.1mm)

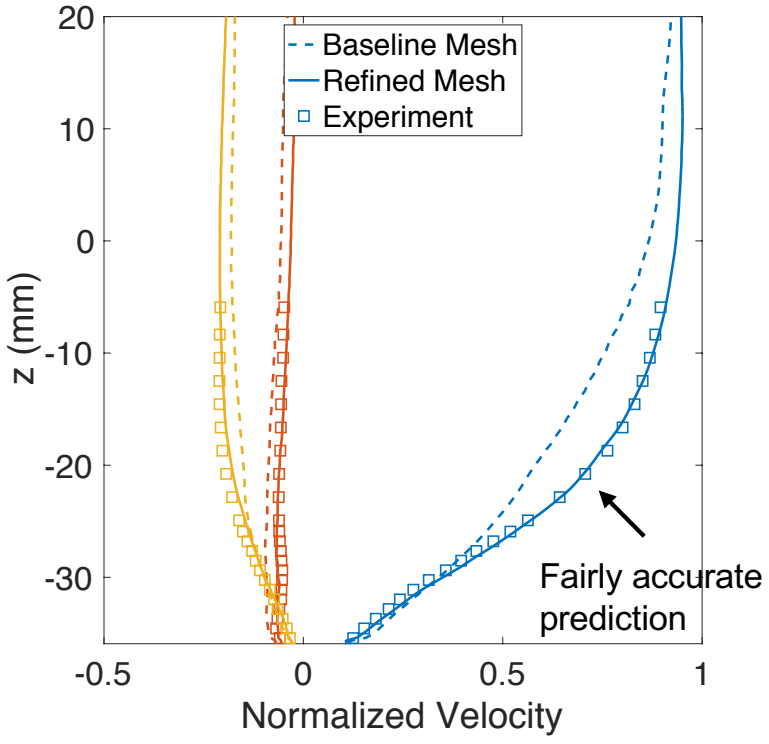
Juncture Probes at x=2952.6mm

WMLES (Sigma SGS model, exchange location=0.5mm)





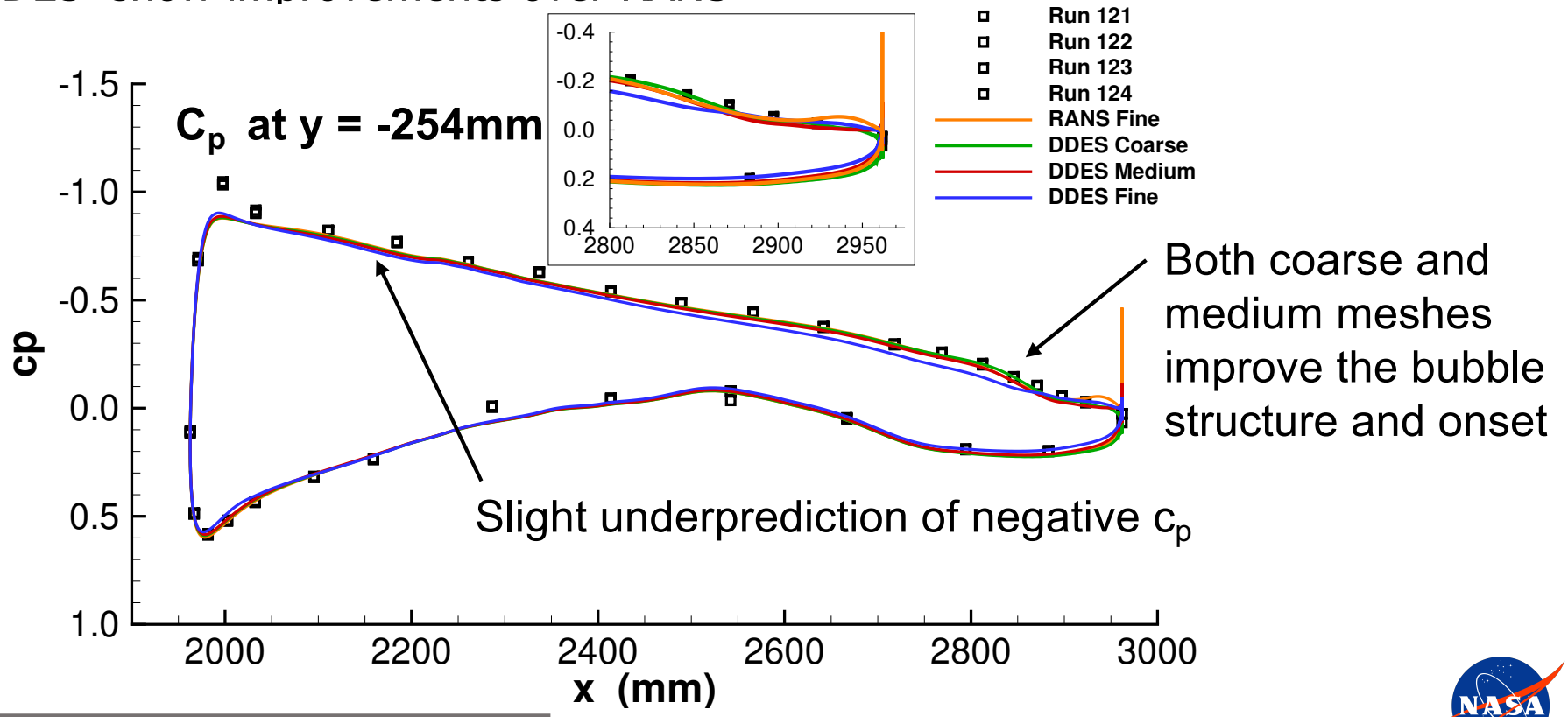
1mm from fuselage wall (y = -237.1mm)



30mm from fuselage wall (y = -266.1mm)

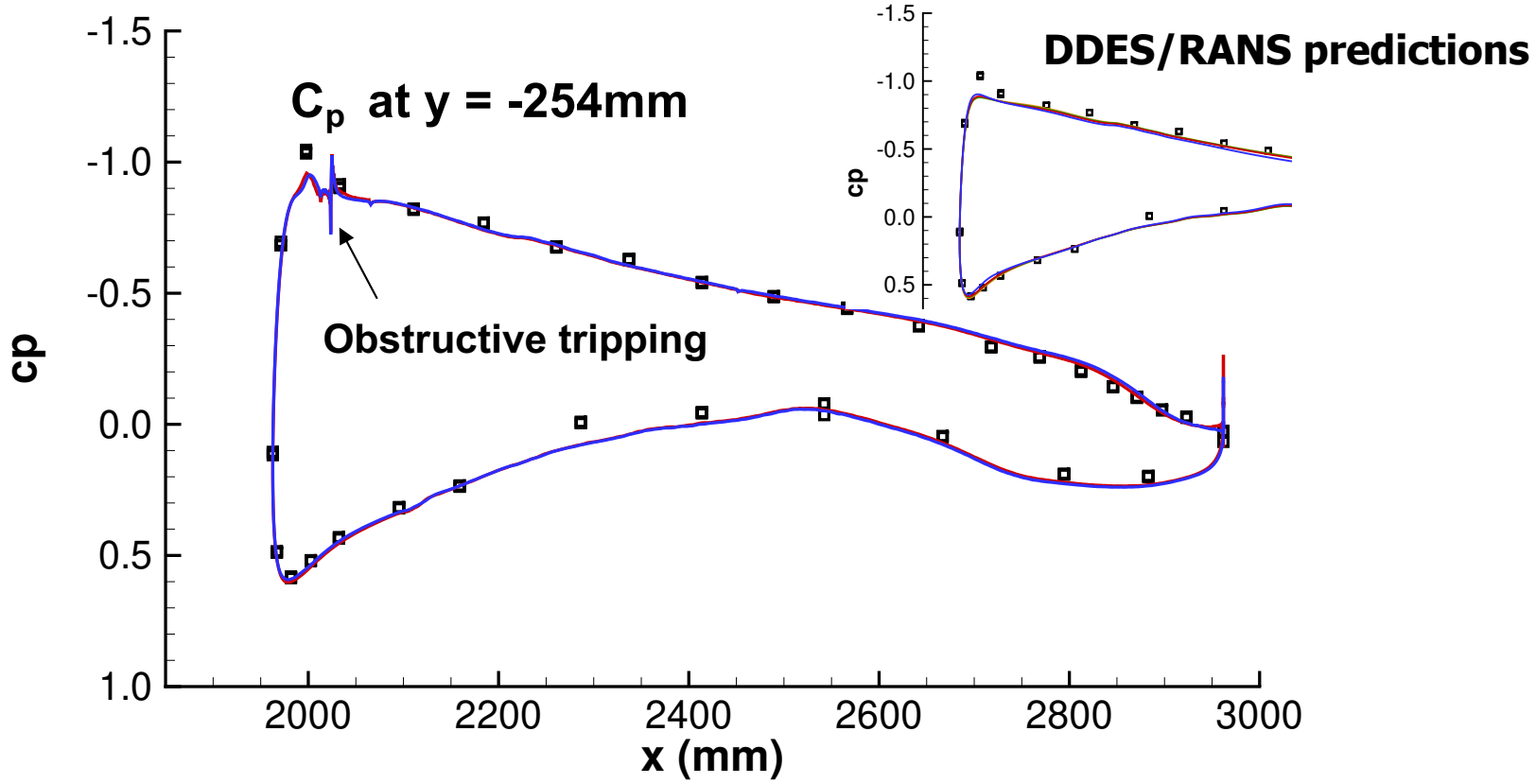
C_p predictions - DDES

Fine mesh DDES predicts early onset of separation but both coarse and medium mesh DDES show improvements over RANS



C_p predictions - WMLES

- Representation of wing-tripping dots changes c_p prediction on suction side

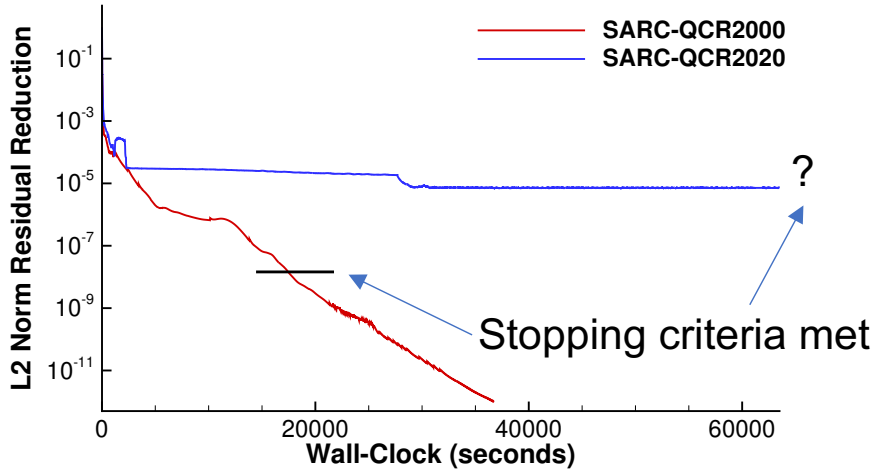


Computational cost

- Steady-state RANS (QCR-2000)

Simulation Type	Timing Criteria	Grid Size	CPU Arch.	Core Hours	NASA SBUs
RANS (Coarse Mesh)	10^{-8} residual reduction	24M	Ivy Bridge	257	8.5
RANS (Medium Mesh)	10^{-8} residual reduction	57M	Ivy Bridge	2216	73
RANS (Fine Mesh)	10^{-8} residual reduction	196M	Ivy Bridge	4889	161

- Additional stiffness with QCR-2020 (Rumsey et al., AIAA J., 2020)



Computational cost

- DDES
  - Initialized from steady-state RANS
  - Initial spin-up for about 5 CTUs and averaged over 20 CTUs

Simulation Type	Timing Criteria	Grid Size	CPU Arch.	Core Hours	NASA SBUs
DDES (Coarse Mesh)	20 CTU	24M	Broadwell	20,060	780
DDES (Medium Mesh)	20 CTU	57M	Broadwell	39,620	1,420
DDES (Fine Mesh)	20 CTU	196M	Broadwell	218,000	7,800

- WMLES
  - Initialized from a WM-RANS steady state to speed up transience and potential flow development
  - Initial spin-up for 7 CTUs and averaged over 20 CTUs (left/right wings serve as two ensembles)

Simulation Type	Timing Criteria	Grid Size	CPU Arch.	Core Hours	NASA SBUs
WMLES	1 CTU (TVD-RK3, Acoustic CFL = 1.4)	520M	Skylake	5500	219
WMLES	1 CTU (BDF2, Incompressible CFL = 1.5)	520M	Skylake	5650	223
WMLES	20 CTU (TVD-RK3, Acoustic CFL = 1.4)	520M	Skylake	110,000	4,380

Summary

- Scale resolving simulations of the juncture flow experiment performed using a) DDES and b) WMLES; comparisons with experiment and RANS SA-RC-QCR2020
- Both WMLES and DDES appear to show improvements over steady-state RANS
- DDES solutions degrade with grid refinement due to modelled stress depletion; the good agreement seen on the medium RANS grids due to fortuitous circumstances
- Lower numerical dissipation appears to improve the DDES results; although marginally
- DDES simulations with QCR-2000 based correction in the underlying RANS is needed to adequately predict separation; SA-RC based DDES predicts early onset of separation
- Velocity profiles from DDES at the outboard LDV location (y=-266.1mm) show large effects of MSD and are inadequate at predicting skin friction
- WMLES profiles show promising agreement with experiment at most outboard LDV probes and the inboard LDV probes just prior to onset of separation
- WMLES shows a persistent streamwise momentum overshoot in the corner (consistent with work by Lozano-Duran et al. (CTR) and Iyer & Malik (NASA Langley)

Summary

- Bubble length predicted by WMLES is smaller than observed (98mm for the refined mesh; 84mm for the baseline mesh)
- Less dissipative Sigma SGS model leads to better results than constant coefficient Vreman model
- Resolution of secondary flow appears to be critical in predicting accurate onset of separation; unclear if only improvements in SGS modeling will help - more resolution is likely needed
- Both DDES and WMLES cost at least an order of magnitude more than LAVA steady state RANS on overset meshes; but comparable with some other steady state RANS reported on O(100M) size meshes
- Results highlight the need for more fundamental canonical test problems to study corner flow separation using WR-LES or DNS

Acknowledgements

- Funded by NASA's Transformational Tools and Technologies (T^3) project under the Aeronautics Research Mission Directorate (ARMD)
- Computer time has been provided by NASA Advanced Supercomputing (NAS) facility
- Authors would also like to thank:
  - James Jensen (ARC) for help with CAD
  - Timothy Sandstrom (ARC) for visualization support
  - Prahladh Iyer (LaRC) for discussions on WMLES
  - Henry Lee (ARC) for providing RANS grids
  - Chris Rumsey (LaRC) and the Juncture Flow committee

Questions?

- Contact information
  - Aditya Ghate (aditya.s.ghate@nasa.gov)
  - Cetin Kiris (cetin.c.kiris@nasa.gov)